IEEE Open Journal of
Power Electronics

Received 27 January 2023; revised 26 February 2023; accepted 28 February 2023. Date of publication 3 March 2023;
date of current version 16 March 2023. The review of this article was arranged by Associate Editor Philip T. Krein.

Digital Object Identifier 10.1109/OJPEL.2023.3251992

On-Board Chargers for High-Voltage Electric Vehicle Powertrains: Future Trends and Challenges

RACHIT PRADHAN (Student Member, IEEE), NILOUFAR KESHMIRI (Student Member, IEEE), AND ALI EMADI (Fellow, IEEE)

McMaster Automotive Resource Centre (MARC), McMaster University, Hamilton, ON L8P 0A6, Canada

CORRESPONDING AUTHOR: RACHIT PRADHAN (e-mail: pradhar@mcmaster.ca)

ABSTRACT The powertrain voltages in battery electric vehicles (BEVs) have witnessed an upward trend due to advantages such as reduced runtime losses and extremely high DC fast charging power levels; aiding in reduced range anxiety and lower battery charging duration. This trend requires original equipment manufacturers (OEMs) to re-assess the design of electronic sub-assemblies (ESAs). Due to newly released DC fast charging standards, there are implications on the on-board charger (OBC), which is one of the ESAs in a BEV. This paper performs a comprehensive review of identifying system-level and use-case related challenges in transitioning on-board chargers to higher voltages compared to state-of-the-art, while considering the impact of newly introduced DC fast charging standards like Megawatt Charging Systems (MCS) and ChaoJi/CHAdeMO 3.0. The existing research in academia and proof-of-concept designs compatible for high-voltage on-board charging sub-systems, such as the power factor correction (PFC) and isolated DC-DC conversion stages is consolidated. Due to the demand for integration driven by cost-optimization targets, single-stage, traction-integrated, and auxiliary power unit (APU) integrated on-board chargers are discussed. Finally, the disparity between state-of-the-art technology and future requirements is defined to establish challenges and the direction of future research areas.

INDEX TERMS Ac-dc converters, battery, dc-dc converters, electric vehicle charging, gallium nitride, high voltage, multilevel converters, silicon carbide.

I. INTRODUCTION

Transportation contributes to 15% of global greenhouse gas (GHG) emissions [1]. An increased degree of electrification provides the highest fuel efficiency improvement, and thus fully electrified BEVs improve the ability to reduce GHG emissions [2]. Compared to gasoline-powered cars, a BEV can reduce GHG emissions by 72% using conventional energy, and 97% by using green (wind, hydro, solar) electricity [3]. Since their conceptualization, most of the established production BEVs have had a battery voltage of 400 V; however, increasing the battery voltage has certain advantages [4], [5]. The average weight of copper consumed in an electric vehicle is 89 kg, about 4.5% of the BEV's total weight [6]. Increasing the battery voltage offers a reduction in the required copper, resulting in reduced conductor size, wiring weight and, thus, an extension in the vehicle's operating range. As opposed to an average refueling time of 3 minutes of an internal combustion engine (ICE) based vehicle, a BEV requires about 25 minutes on average with charging powers up to 400 kW [7]. Since the average amount of time required to fast charge a BEV is 8.3 times higher than that of an ICE vehicle, this is a major barrier to the mass adoption of BEVs [8]. Increasing the battery voltage enables faster DC fast charging without increasing the size of the charging cable, while delivering higher power, which is one major factor in driving high-voltage electrification.

A comprehensive study of various AC-DC and DC-DC converter topologies for conductive and inductive charging applications has been performed in [9]. Global standards governing DC fast and on-board charging, and their implication

on the vehicle architecture and its components have been reviewed in [10]. Introduction of bi-directional on-board charging and the opportunities enabled by vehicle-to-everything (V2X) connectivity features have also been addressed [11]. The studies performed in previous literature are applicable to BEVs with powertrain voltages <1 kV. A review of existing and newly introduced DC fast charging standards, with charging connector voltages >1 kV are performed in [7], [12]. Introduction of new high-voltage DC fast charging standards impact the architecture and design choices of the on-board charger in an electric vehicle due to its dependency on the battery pack voltage. There are plausible merits of increasing the battery pack voltage for the next-generation of electric vehicles. However, the implications of increasing the battery pack voltage on the vehicle's on-board charger have not been addressed in literature. This paper aims to consolidate the barriers in increasing the battery voltage beyond existing voltage levels from the vehicle's, charging infrastructure's and upcoming regulatory standards' viewpoint. It also aims to review viable AC-DC converters, DC-DC converters, and integrated on-board charger topologies to address challenges concerning on-board chargers in BEVs with high-voltage powertrains.

This paper is organized as follows. Section II discusses the different types of BEV charging methods, and the basics around each method have been established. The reason for the mass adoption of on-board charging as an essential charging method is defined. Section III discusses the trend of increasing battery voltage in the BEV market. The 800 V vehicle class has witnessed mass adoption, and the voltage limits of existing DC fast charging connectors are being approached. An attempt to project the upper voltage limits in defining the next-generation class of BEVs is made, and challenges and implications of scaling the battery voltage are discussed. The use cases of increased battery voltages based on state-of-the-art thermal limitations are inferred. In Section IV, the high-level geographical distribution of voltage, power levels, and connector types are discussed to establish the interoperability-related challenges. Next, use cases are developed in order to understand the co-dependency of DC fast charging and on-board charging systems, to further clarify the direction of mass adoption of the discussed voltage levels, and, to identify their bottlenecks. In Section V, the sub-systems in a two-stage high-voltage on-board charger are discussed. Various topologies for the three-phase AC-DC i.e., the power factor correction (PFC) stage and the isolated DC-DC conversion stage, are discussed. The required regulatory compliance requirements for various aspects of the development of on-board chargers are covered. Section VI discusses various topologies of single-stage on-board chargers, traction-integrated on-board chargers, and auxiliary power unit (APU) integrated on-board chargers. In Section VII, the current gap in state-of-the-art power electronics to comply with the upcoming voltage levels and their relevant research directions are summarized. Section VII contains concluding remarks.

II. ELECTRIC VEHICLE CHARGING

To meet the electric vehicle (EV) market goals set by the Global EV Outlook and governments around the world, expansion of the charging infrastructure is necessary. In 2021, the number of publicly available EV charging stations increased by 41% [13]. EV chargers fall under three categories: DC fast charging, on-board charging, and wireless charging. In this Section, a brief introduction to various charging methods is discussed.

A. DC FAST CHARGING

DC fast charging permits the EV to be fully charged in less than an hour. Fast charging stations are installed on highway rest areas over the US and cities in North America and Europe, similar to a gas station. These systems typically derive power from the grid at voltages of 380 V or higher [12]. These chargers are off-board, meaning they require external installation and infrastructure. Since Level 3 chargers operate at higher power levels (50 kW and higher), the chargers are larger in size, leading to the need for off-board infrastructure. Public stations typically use Level 2 or 3 chargers to permit rapid charging. However, high-power charging can increase the demand on the grid, impacting the local distribution infrastructure, especially at peak times [14]. In this case, a lower charge power is beneficial to minimize peak time impact. Since DC fast charging is analogous to filling the tank of an ICE vehicle, this method is the most appealing to consumers, in terms of convenience and efficiency. However, the higher cost associated with DC fast chargers and the long-term impact on the battery's state of health (SOH) act as a deterrent for some consumers from using these chargers [15]. Another drawback associated with fast chargers is the scarcity of DC fast charging infrastructure and the resultant range anxiety.

B. CONDUCTIVE ON-BOARD CHARGING

The on-board charger is an electronic sub-assembly (ESA) of the vehicle and is classified into Level 1/ Level 2/ Level 3 AC charging, and can be bidirectional or unidirectional in nature. Unidirectional charging from the grid to the EV is the most common type of charging. This method reduces the hardware requirements and lowers the cost. Battery degradation is also reduced with unidirectional charging, extending the battery lifetime [16]. Bidirectional charging permits charging of the EV from the grid while enabling power flow back to the grid from the EV battery, i.e. V2X operation. With on-board chargers, the power level is limited due to cost, space, and weight limitations. Integration of the OBC with the electric drive enables the design of power dense solutions [16]. OBCs can be further categorized into inductive and conductive chargers. Charging through direct contact between the charge inlet and connector is referred to as conductive on-board charging. The process through which power is transferred magnetically is known as inductively coupled on-board charging. Compared to DC fast chargers, an OBC permits the EV owner to charge their vehicle overnight at the convenience of their home. Since charging typically occurs outside of peak hours (overnight),

the net cost of on-board charging is lower than that of DC fast charging. The risk of battery degradation is also reduced due to lower C-rates encountered by the battery pack [17].

C. INDUCTIVE (WIRELESS) ON-BOARD CHARGING

In recent years, wireless charging has gained a lot of attention. As with consumer products, wireless charging of an EV permits more convenient charging. This process occurs via inductive coupling, where the electric current passing through a coil creates a magnetic field, transferring power between the primary and secondary coils [18]. Wireless charging is categorized into two sub-types: static and dynamic wireless charging. Static wireless charging is enabled using installation of dedicated wireless charging pads at rest stops or parking lots, and is applied for stationary vehicles. It is a direct replacement for conductive on-board charging, without the risk of isolation faults between the grid and the battery pack due to the lack of a conductive interface between the charger and the vehicle [19]. Dynamic wireless charging is a futuristic charging method, that is associated with high infrastructure installation costs. It utilizes charging pads embedded inside the road and charges the vehicle while it has momentum. Dynamic wireless charging enables battery pack size reduction. However, it is challenging to maintain high system efficiency due to concerns of misalignment between the transmitter and receiver coils [20].

D. CHARGING TRENDS

The total number of publicly available fast chargers was about four times that of publicly available slow chargers, from 2015-2021 [21]. There are increasing concerns about the stability of the grid with the increased use of DC fast charging [22], [23], [24], [25]. The low cost of residential electricity versus the infrastructure cost of public charging stations as well as the cost of gas, makes home charging the most affordable charging option. In Canada, the cost comparison between OBC and DC fast chargers can be summarized as below [26]:

- In Quebec, the use of OBC is 30% less expensive than DC fast chargers and six times less expensive for driving 62 miles on electricity as opposed to gas.
- In Ontario, it is 65% less expensive to use an OBC than a DC fast charger and five times less expensive to drive 62 miles on electricity versus gas.
- In British Columbia, it is 30% cheaper to charge at home compared to using a fast charger and five times less expensive to drive 62 miles on electricity versus gas.

A consumer case study performed by Morrissey et al. shows that peak usage of DC fast charging happens in the evening, while it happens in the afternoon and night for the standard charging (on-board charging) [27]. When consumers park their vehicles, on-board charging is more suitable since there is ample time to top-up the vehicle. This data suggests that most EV consumers prefer on-board charging, and this trend is expected to stay the same, with increased deployment of DC fast chargers, due to the cost incentive of using on-board chargers.

III. INCREASING BATTERY PACK VOLTAGE

In a BEV, the high-voltage (HV) battery pack is the primary and sole source of energy for both propulsion and auxiliary functions of the vehicle. The battery pack is typically constructed using a combination of paralleled and serialized Lithium-ion (Li-ion) cells. The cell configuration is generally denoted as $XsYp$, where X is the number of series-connected cells, and Y is the number of parallel-connected cells used to form the battery pack. There has been a general trend of vehicle manufacturers increasing the battery pack voltage. A high-voltage battery pack reduces the current required to transfer the same power at a lower voltage and thus offers benefits such as lower run-time ohmic losses, very low DC fast charging duration, and reduction in the overall weight of the powertrain conductors. Table 1 consolidates a list of production BEVs (Sedans) sorted as per their release/serial production date, indicating the above-mentioned trend of increasing battery pack voltages [28], [29], [30], [31], [32], [33], [34], [35], [36], [37], [38].

A. CELL CHEMISTRY OPTIONS

The Li-ion cell is the most used cell type for construction of BEV battery packs. There are multiple cell chemistry sub-types of Li-ion cells, such as Lithium Titanate Oxide (LTO), Lithium Iron Phosphate (LFP), Lithium Nickel Manganese Oxide (NMC), Lithium Cobalt Oxide (LCO), Lithium Manganese Oxide (LMO), Lithium Nickel Cobalt Aluminum Oxide (NCA). Table 2 summarizes the key characteristics of these cell chemistries such as the voltage range, energy density, cell life, and thermal runaway temperatures, that are also deciding factors for its application in a BEV [39]. As of 2020, NMC and LFP cell chemistries dominate the market share of cell chemistries used in electric vehicle applications [40]. Adoption of NMC cells is driven by its high energy density and life cycles, whereas for the LFP cell type it is driven by its stability and high life cycles. A comparison between 18650 and 21700 cells is done by Waldmann et al.; it concludes that the energy density increases by approximately 6% for the 21700 cells [41]. It is seen from Table 1 that the market is also moving away from 18650 cells to 21700 cells in its latest vehicles, due to its increased energy density. Furthermore, Tesla has introduced the 4680 cell, which lowers the number of cells required to manufacture the battery pack, resulting in a reduced production cost. However, data regarding the cell's field performance is unavailable due to its nascent stage. Non-aqueous Lithium-air cells are a promising cell technology since the electrolyte in a conventional lithium-ion cell is replaced by air, thus increasing its power density. Targeted power densities for Lithium-air cells are set to 13 kWh, but since they are air-breathing cells, performance is dependent on the air quality of its application [42]. Solid-state Li-ion cells have the potential to reach energy densities up to 300 Wh/kg, two-three times the existing technologies such as LFP or NMC [43].

TABLE 1. List of BEVs (Sedans) in Production Indicating Their Li-Ion Battery Voltages, Capacities, and OBC Power levels [28], [29], [30], [31], [32], [33], [34], [35], [36], [37], [38]

Vehicle	Release	Origin	Max. Battery Voltage (V)	Cell	Cell Config.	Battery Capacity (kWh)	OBC Power Level (kW)	≈ Charge Time
Lucid Air Touring	2022	U.S	756	21700	180s30p	93	19.2	4h 51m
Audi e-Tron GT	2021	Germany	832	Pouch	198s2p	93	11*	8h 27m
Lucid Air Dream	2021	U.S	924	21700	220s30p	118	19.2	6h 09m
BYD Han	2020	China	420	BYD Blade	115s1p	76.9	6.6	11h 39m
Porsche Taycan Turbo S	2019	Germany	832	Pouch	198s2p	93.4	11*	8h 30m
Porsche Taycan	2019	Germany	706	Pouch	168s2p	79.2	11*	7h 12m
Tesla Model 3 LR	2018	U.S	403	21700	96s31p	82	11	7h 27m

* 22 kW power level is available as an optional upgrade. The default power level of 11 kW is specified.

TABLE 2. Summary of Li-Ion Cell Chemistry Types

Cell Chemistry	Voltage Range	Energy Density (Wh/kg)	Life (cycles)	Thermal Runaway
LTO	1.8-2.85 V	70-80	3000-7000	150°C
LFP	2.5-3.65 V	90-120	1000-2000	270°C
NMC	3-4.2 V	150-220	1000-2000	210°C
LCO	3-4.2 V	150-200	500-1000	150°C
LMO	2.5-4.2 V	100-150	300-700	250°C
NCA	3-4.2 V	200-260	500	150°C

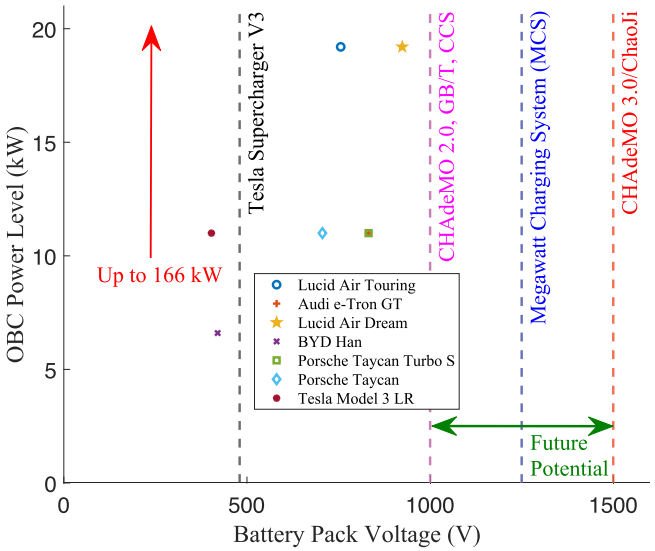

FIGURE 1. Current status of battery voltage and OBC power levels of BEVs in comparison to the DC fast charging connector voltage limits.

B. PROJECTING THE UPPER BATTERY VOLTAGE LIMITS

The first standard indicating the connector specifications of a conductive coupling-based charging method was established in 2001 with the standard SAE J1772-2001 [44]. The first serial production BEV with a Li-ion battery pack was a Tesla Roadster, released in 2008 [45], seven years after the connector specification was first defined. Tesla and other consortiums have established their own charging standards as the BEV landscape evolved. Historically, the charging connector specification has attempted to be standardized ahead of its vehicle production timeline. Based on a study in the U.K., DC fast charging installations have seen an average year-on-year (YoY) increase of 35% [46], indicating a heavy push to fast charging infrastructure. The U.S. Department of Transportation (U.S. DOT) and U.S. Department of Energy (U.S. DOE) have committed $5 Billion towards building a national EV charging network under the National Electric Vehicle Infrastructure (NEVI) formula program [47]. With ample capital expenditure budgets towards charging infrastructure, on-road and upcoming BEVs are required to be compatible with the specifications of DC fast charging infrastructure.

The charging connector standards indicating the DC fast charging levels implemented worldwide have been listed in [7], [12]. As of 2022, the highest voltage offered by any DC fast charging connector is via the CHAdeMO 2.0 or CCS Combo 2 at 1000 V. The 2021 Lucid Air Dream has a battery operating at a maximum of 924 V, which is indicative of saturation towards the upper voltage limit offered by existing DC fast charging connectors [28]. In addition, regional variations of the charging connectors introduce additional stock-keeping units (SKUs) in a vehicle's grid-interface components and increase the cost overheads experienced by an Original Equipment Manufacturer (OEM), which percolates to the user. CharIN has defined the specifications of the Megawatt Charging System (MCS) capable of delivering up to 3.75 MW of power (1.25 kV/ 3000 A) and is intended for global adoption for DC fast charging of trucks, buses, and perhaps aerospace, marine, and mining equipment as well [48]. This standard is also proposed for harmonization under SAE J3271, which is currently under development [49]. In Japan and China, the CHAdeMO 3.0/ChaoJi standard can provide DC fast charging up to 900 kW (1.5 kV/ 600 A) [50]. The definition of this standard opens up possibilities of increasing the battery pack's voltage level beyond the existing limit of 1 kV [51].

Fig. 1 shows a graphical representation of the battery pack voltages and OBC power levels of the vehicles discussed in Table 1. The voltages of the battery pack have been compared against existing and upcoming DC fast charging connector

TABLE 3. >1 kV DC Fast Charging Connector Specifications

DC fast charging Connector	Region	Voltage (V)	Current (A)	Power (kW)
CHAdeMO 3.0 / ChaoJi	Japan, China	1500	600	900
Megawatt Charging System (MCS)	North America, E.U	1250	3000	3750

capabilities [12], [50]. It can be observed that the battery voltages of all vehicles in production are currently limited to 1 kV. The introduction of DC fast charging standards such as MCS and ChaoJi enable extension of the vehicle's battery pack voltages, where 1 kV $< V_{batt} <$ 1.5 kV, thus aiding in increased DC fast charging capability. Additionally, AC Level 3 charging with power levels up to 166 kW can be explored. The voltage and current specifications of the high-voltage DC fast charging connectors ($V_{batt} >$ 1 kV) are summarized in Table 3.

C. CHALLENGES IN SCALING THE BATTERY VOLTAGE

A high serialized cell count is required to increase the battery pack voltage. Based on the type of vehicle (Sedan/Hatchback/SUV/Van/Bus), the volume available for the battery pack is fixed. Increasing the allocated battery pack volume can compromise product-level features such as available passenger space, or reduction in maximum attainable speed. From Table 1, it can be observed that the general battery pack capacity of Sedans lies between 77–94 kWh, with an exception of Lucid Air Dream, which is the high-range variant of Lucid Air [28]. With the limit of the battery pack capacity in battery-operated Sedans being well established, a similar consolidation shall be foreseen in other vehicle types. Based on the existing cell configurations and in-production cells, a reconfiguration can be performed to increase the battery voltage, however, the following challenges are observed:

- Due to increased voltage, additional clearance and creepage distance are required to avoid insulation failure/partial discharge, while meeting the battery safety requirements as per UL 2580 [52]. This consumes unused volume in the battery pack's chassis and packaging the same number of cells as the lower voltage battery pack may not be possible.
- Scaling the voltage up to 1.5 kV requires reconfiguration of the cell count such that existing battery packs have their parallel cell count reduced, and serial cell count increased to achieve the desired string voltage. This is possible in cases where parallelling is performed, unlike the BYD Han, which utilizes the BYD Blade cell in a 1p configuration [33].
- The battery management system (BMS), which is responsible for the safety and state estimation of the battery, generally follows a functional safety development cycle, recommended by ISO 26262 due to its safety-critcal role in the vehicle powertrain [53], [54]. Measurements such as redundant battery string voltage and contactor weld detection circuits require isolation amplifiers with enhanced isolation to maintain isolation between the low-voltage and high-voltage circuitry [55].
- The high-voltage battery has a redundant disconnect mechanism as a functional safety requirement. The chemical pyrofuse is activated when the contactors are unable to open the battery circuit in the event of a critical safety violation. The contactors are typically realized using the white-labeled versions of the TE Connectivity KILOVAC/GIGAVAC/EVC series automotive contactors, which are rated up to a maximum voltage of 900 V among all the above-mentioned series [56]. Switchgear manufacturers would require to work with OEMs to develop and validate a high-voltage series of automotive contactors and fuses to support voltages up to 1.5 kV.

D. IMPLICATION ON POWERTRAIN COMPONENTS

A BEV powertrain consists of components such as the high-voltage battery pack, BMS, traction inverter, propulsion motor, and auxiliary power unit (APU) [57]. The challenges in scaling battery voltage, and its implication on the high-voltage battery pack and the BMS have been discussed in Section II-III-C. Depending upon the power level to be catered to, increased voltage stresses on the traction inverter may require use of multilevel inverter topologies such as the T-type inverter or active neutral-point clamped (ANPC) inverter to reduce switching losses [58], [59]. Increasing the number of levels comes at the disadvantage of added cost and lower specific power in a market that is already very sensitive to cost. However, multilevel inverters enjoy benefits such as lower voltage total harmonic distortion (THD), electromagnetic interference (EMI), and higher efficiency at higher voltages [60], [61]. Furthermore, advanced modulation techniques can be implemented in multilevel traction inverters to improve their power density without changing modification in their construction [62]. At higher voltages, the base speed of the propulsion motor increases, thus extending the reach of the torque-speed envelope [63]. For a higher voltage and same power, the conductor sizing of the motor would reduce, with an opportunity to reduce the conduction losses. A comparison between a 500 V and 650 V Toyota Prius motor shows 45% improvement in the motor's specific power, which makes a strong case for higher voltage motors [64]. The APU is the link between the high-voltage battery pack and the low-voltage loads such as the car computer, infotainment system, actuators, and cooling pumps. Isolation between the two ports of the APU is mandatory due to the safety risks to a passenger from exposure to high-voltage, and thus requires higher insulation co-ordination within the APU. For the same

power level, high-voltage switches experience lower current stress, but an overall increase in the cost of the APU [4], [65].

E. APPLICATIONS OF > 1 KV BATTERY VOLTAGE

The list of existing DC fast charging standards and their respective charging connector current and voltage limits are discussed by the authors in [7]. As the voltage increases, the ability to deliver higher power at a particular current limit increases. This will vary the C-rates at which the battery packs are being charged.

$$E_{batt(kWh)} = 400\ V.B_{cap(Ah)} = 1500\ V.\left(\frac{B_{cap(Ah)}}{3.75}\right) \quad (1)$$

To portray the impact of varying C-rates, a comparison between 400 V and 1500 V systems is made. As highlighted in the previous subsection, the maximum C-rates for a Tesla Model 3 vary between 2.6 C-3.3 C at a charging power of 195-250 kW. The total energy capacity of the battery pack $E_{batt(kWh)}$ is achieved by having a battery capacity of $B_{cap(Ah)}$ for a 400 V system, as seen in (1). In the case of a 1500 V system, the same energy capacity is achievable by having a battery capacity of $\frac{B_{cap(Ah)}}{3.75}$. Under a case where the resultant charging currents are the same (almost one fourth the charging power at 400 V compared to 1500 V), the C-rates for an assumed energy capacity of a battery will be 3.75 times at the 1500 V bus voltage level. Maintaining a moderate temperature rise at the higher C-rates will increase challenges on the thermal management significantly [71]. This means that as the battery pack voltage increases, it would be imperative to increase the battery pack capacity to keep the thermal management reasonable at higher power levels. As seen in Table 1, the average battery capacity of BEV Sedans is approximately 90 kWh. With increased voltage levels, and to fully utilize the benefits of higher voltage charging while maintaining existing C-rates, the battery pack capacity is required to be at least 4x, i.e. 360 kWh. If the C-rates of the battery pack are otherwise increased, it will cause a higher cell temperature rise. Increasing the cell temperature has a detrimental impact on the life of the cells. A study performed by M. Uitz et al. on Tesla's 18650 cells shows that the capacity fading of these cells after 500 cycles is 30% at 60 °C as compared to 20% at 25 °C [72]. Proportionately increasing the battery capacity will thus ensure that the life of the battery pack does not experience significant degradation, provided the necessary cooling is achieved after increasing its size. This also aligns with the motivation of introducing the MCS and CHAdeMO 3.0/ChaoJi standard, that was to cater the medium to heavy vehicles DC fast charging segment. Table 4 shows the battery voltages and capacities of medium and heavy duty vehicles that are in production and due for release [66], [67], [68], [69], [70]. It can be observed that the battery capacities lie in the > 300 kWh range. The voltages, however are still in the < 1 kV range due to large deployment of CCS compliant DC fast chargers, lack of a charging connector standardization, and a lack of maturity of high-voltage DC fast charging standards [73].

TABLE 4. Battery Specifications of Medium to Heavy-Duty BEVs [66], [67], [68], [69], [70]

Vehicle	Vehicle Type	Origin	Battery Voltage (V)	Battery Capacity (kWh)
Nikola Tre	Semi-Truck	U.S	800	753
Tesla Semi (300)	Class 8	U.S	800	≈ 600
Tesla Semi (500)	Class 8	U.S	800	≈ 1000
BYD K9M	40' Bus	China	693	313
BYD K11M	60' Bus	China	-	578
Scania Electric Truck	Electric Truck	Sweden	650	624

IV. HV ON-BOARD CHARGING CHALLENGES

This Section discusses an overview of high-voltage conductive on-board chargers. At first, the geographical variation of the grid voltages, and standard adoptions are discussed to set the regional voltage, and power level baselines. Under increasing voltages, the co-dependency between conductive on-board charging and DC fast charging under various application scenarios is presented. Finally, use case related challenges in scaling up the voltages are summarized.

A. POWER LEVEL CLASSIFICATION

The three key markets in the world with high penetration of BEVs are the United States (U.S), European Union (EU), and China. Their regional electrical transmission networks operate at unique and incompatible voltage levels, which drives the power-conversion stage design based on regional need. It is notable that the EU and China have similar operating voltages, and hence the OBC can be designed for inter-compatibility between these regions. As discussed in Section II, on-board charging can be classified into three levels (Level 1 - Level 3), for which a summary of regional, voltage and power level classification is shown in Table 5.

1) AC LEVEL 1 (L1) CHARGING (< 3.7 KW)

This level is used in cases where very slow charging is acceptable. The general charging duration for a full charge varies between 3-4 days depending upon the power level and the vehicle's battery capacity. The United States supports two connectors for L1 charging, the SAE J1772 and the Tesla proprietary connector. As per SAE J1772, 1.92 kW L1 charging can be supported with a 120 V/16 A single-phase supply [74]. The Tesla proprietary connector supports a 1.4 kW L1 charging level with its mobile connector that plugs into a standard NEMA 5-15 wall outlet, drawing 12 A from a 120 V single-phase supply [75]. The L1 charging specification is not applicable to the EU and China.

2) AC LEVEL 2 (L2) CHARGING (3.7–22 KW)

This level is used in cases where the vehicle is required to be fully charged under a 7-8 h charging use case. In the United

TABLE 5. Regional, Voltage, and Power Based Classification of OBCs

SAE J1772 Level	Connector	Voltage (V)	Current (A)	Power (kW)
North America				
AC Level-1 3.7 kW	J1772	1 Φ 120	16	1.92
	Tesla	1 Φ 120	12	1.4
AC Level-2 3.7-22 kW	J1772	3 Φ V_{LL} 208	80	16.6
		Split 1Φ 240	80	19.2
	Tesla	Split 1Φ 240	48	11.5
AC Level-3*	IEC 62196 Type 2	3 Φ 208Y/120	63/160†	22.7/57.6
		3 Φ 480Y/277	63/160†	52.3/133
		3 Φ 600Y/347	63/160†	65.6/166.5
Europe				
AC Level-1 3.7 kW	-	-	-	-
AC Level-2 3.7-22 kW	IEC 62196 Type 2	1 Φ 230	32	7.36
	IEC 62196 Type 2	3 Φ 400Y/230	32	22
AC Level-3 22-43.5 kW	IEC 62196 Type 2	3 Φ 400Y/230	63	43.5
China				
AC Level-1 3.7 kW	-	-	-	-
AC Level-2 3.7-22 kW	GB/T 20234 AC	1 Φ 220	32	7.04
		3 Φ 380Y/220	32	21.12
AC Level-3 22-43.5 kW	GB/T 20234 AC	3 Φ 380Y/220	64	40.92

* SAE J1772 was never implemented for L3 charging in the U.S, and was replaced by SAE J3068 [78]

† Maximum amperage of the Advanced Contact defined under SAE J3068.

States, both the SAE J1772 and Tesla connectors support L2 charging up to 19.2 kW [74] and 11.5 kW [38] when powered up using a 240 V single phase (1 Φ) supply. In installation cases where the power is drawn between two phases of a three-phase (3 Φ) Wye-connected rail, the available voltage is 208 V, and the power is limited to 16.6 kW, within the specification of SAE J1772. Tesla's OBC does not support the 208 V voltage level. In the EU, charging is supported by the IEC 62196 Type 2 connector. With 1 Φ 230 V, the power level is limited to 7.36 kW, while at 3 Φ 400 V, a charging power of 22 kW can be achieved. This power is limited by the connector contact's current rating of 32 A [76]. In China, the GB/T 20234 AC connector supports L2 charging. With 1 Φ 220 V, the power level is limited to 7.04 kW, while at 3 Φ 380 V, a charging power of 21.12 kW can be achieved. This power is also limited by the connector contact's current rating of 32 A [77].

3) AC LEVEL 3 (L3) CHARGING (22–166 KW)

This level was originally considered for a range of 22–43.5 kW by the SAE J1772 standard, however was never implemented for light vehicles. As per Appendix M of the SAE J1772 standard, the SAE J3068 standard was referred for the development of three-phase on-board charging for medium to heavy-duty vehicles [74]. Since the SAE J1772 connector does not support three-phase charging, a modification of the IEC 62196-2 connector has been proposed for use under the SAE J3068 standard for use in North America [78]. The 3 Φ supply is available at distinct voltage levels such as 208/480/600 line-line voltage (V_{LL}). The power level is limited by the current capability of the IEC standard contacts at 63 A. SAE J3068 has also defined advanced contacts of 100 A, 120 A, and 160 A to further increase the power delivery to the OBC when heavy-duty vehicles such as buses, trucks, industrial machinery are manufactured with large battery packs. In the EU and China, the OBC levels are restricted to 43.5 kW and 40.92 kW, as originally defined under SAE J1772.

B. CO-DEPENDENCY OF DC FAST AND ON-BOARD CHARGING VOLTAGE LEVELS

As discussed in Section II-B, the DC fast charging connector specification is one of the most significant factor in driving the battery voltage limits of a vehicle. The available on-board charging power is determined by the limits of the AC charging connector, which varies based on the geographical region of operation. The AC and DC fast charging connectors are often integrated into one connector (such as the CCS Combo). For moving to higher voltage levels, identifying the points of interaction betweeen DC fast and on-board charging is required. Fig. 2 discusses the various architectures and their relevant use cases that can be expected as an interaction between DC fast charging and conductive on-board charging.

1) < 1 KV BATTERY WITH A LOWER VOLTAGE DC FAST CHARGER

The configuration shown in Fig. 2(a) is representative of a case to support a DC fast charger with a lower voltage compared to the battery pack voltage. An intermediate stage of DC-DC conversion is required to match the voltage of the DC fast charger with that of the battery. In this case, the battery voltage range is 400 V–1 kV, and the DC fast charger is rated up to 400 V. Matching the voltage between the output of the DC fast charger and the battery pack is typically achieved by operating the OBC in the DC-DC conversion mode. This can be done by bypassing the PFC stage, and only utilizing the DC-DC converter in the OBC. Lucid Air has this support for legacy 400 V chargers for its 924 V battery voltage, enabling legacy charging up to 50 kW due the 'Wunderbox,' which acts as an active front end [79]. Vicor Power has launched the NBM6123, which is a 6 kW power module with a peak efficiency of 99.3% for assisting compatibility between 400 V DC fast charger and 800 V BEV architectures [80]. Matching the power level of the on-board DC-DC converter to that of the DC fast charger (up to 400 kW) is unrealistic due to associated cost and added weight in the vehicle. Due to this reason, the DC fast charging power is limited to the power level of the on-board DC-DC converter, and is the drawback of this use case.

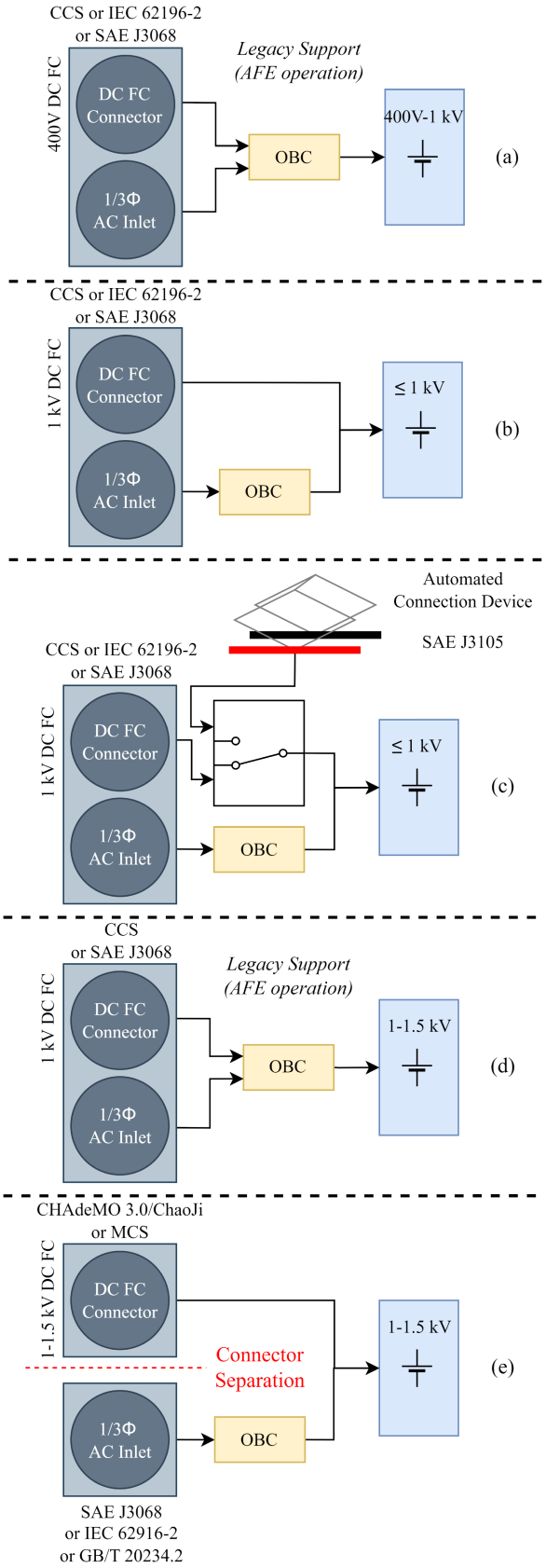

FIGURE 2. Co-dependency scenarios of DC fast and on-board charging.

2) < 1 KV BATTERY WITH A COMPATIBLE DC FAST CHARGER

The configuration shown in Fig. 2(b) is representative of a case to support a DC fast charger that is compatible with the battery pack voltage (<1 kV). The support of both 400 V and 800 V class vehicles can be done with the use of a wide-output voltage DC fast charger [81]. No additional DC-DC conversion stages are required in the case of DC fast charging, and hence charging power level is not compromised. CCS and SAE J3068, both have a DC connector voltage specification of 1 kV, and hence the battery voltage is limited by it. The charging infrastructure is currently tackling the inter-compatibility issue between 400 V and 800 V class vehicles [4], [82].

3) < 1 KV BATTERY WITH A COMPATIBLE DC FAST CHARGER AND AUTOMATED CONNECTION DEVICE (ACD) SUPPORT

The SAE J3105 standard defines the electrical and physical properties of an Automated Connection Device (ACD), that is used to enable conductive charging via an overhead pantograph [83]. The voltage level of this standard also matches that of CCS and SAE J3068, which is why the architecture represented in Fig. 2(c) integrates an ACD network upon the architecture defined in Fig. 2(b). Since the voltage levels are compatible, the ACD can be integrated by having a selection path between the DC fast charging and ACD input being routed to the battery pack [84].

4) 1-1.5 KV BATTERY WITH A LOWER VOLTAGE DC FAST CHARGER

This use case is similar to the one shown in Fig. 2(b), with a difference being rated at a higher voltage. As seen in [21], the number of publicly available DC fast charging stations is increasing, and there is a large deployment of CCS compliant charging stations for light vehicles. It is also discussed in Section III-E that higher voltage powertrains would be advisable for medium to heavy-duty vehicles. The parking locations differ in size between light and medium to heavy-duty vehicles [85]. Due to this reason, the existing charging infrastructure would not be applicable for for higher voltage vehicle applications. Tesla Megachargers are being installed to support the charging of Tesla Semi [86]. To utilize the full potential of DC fast charging, the on-board DC-DC converter used to match the voltage level is required to be sized for the full power level, which is not feasible. Due to these reasons, the likelihood of mass adoption of the charging architecture shown in Fig. 2(d) as a long term solution is not viable.

5) 1-1.5 KV BATTERY WITH INDEPENDENT ON-BOARD AND DC FAST CHARGING CONNECTORS

Both CCS and the combined AC and DC connector of SAE J3068 are limited up to 1 kV operation from the DC connector's specification. This is a major barrier in increasing the battery voltage beyond 1 kV for medium or heavy-duty vehicles, for which SAE J3068 is also the intended on-board

TABLE 6. Potential Regional Combination of AC Level 3 and DC Fast Charging Connectors

Region	AC L3 charging connector	DC fast charging connector	Max. Battery Voltage (V)
North America	SAE J3068	MCS	1250
Europe	IEC 62196-2	MCS	1250
Japan/ China	GB/T 20234 AC	CHAdeMO 3.0/ ChaoJi	1500

charging standard. The SAE J3068 charging connector is a derivative of the IEC 62196-2 connector system, which is a reason for this limitation. Higher voltages cannot be achieved without changes in the connector geometry to accommodate suitable creepage and clearance limits for higher voltages [87]. The architecture shown in Fig. 2(e) relies upon separated AC charging and DC charging connectors. AC Level 3 charging has a possibility to be scaled up to 166 kW. DC charging can be scaled up to 3.75 MW via the MCS, and 900 kW via CHAdeMO 3.0/ChaoJi, and there is no combined AC and DC charging connector currently planned. Taking an example of DC fast charging at 900 kW/ 1.5 kV, the current rating is 600 A. The weight of a compatible 1.5 m DC fast charging cable will be about 26 kg [4]. Management of cable weight in combining a connector for both the DC fast and AC Level 3 charging power levels will be challenging, and thus acts as a catalyst to separate the charging connectors. Based on the planned region of operation, Table 6 discusses the possible combination of the AC Level 3 and DC fast charging connector and their relevant battery voltages.

V. HV ON-BOARD CHARGER SUB-SYSTEMS

In this Section, the sub-systems of a two-stage on-board charger have been discussed. Possible candidates of the AC-DC converter stage i.e the power factor correction (PFC) and the DC-DC converter stage have been presented. A consolidated comparison of all the relevant topologies has been discussed for each converter type.

A. POWER FACTOR CORRECTION (PFC) STAGE

The PFC stage is encountered at the grid interface. It is required since the conventional AC-DC converters (rectifiers) lead to a poor power factor, and manifest as issues such as harmonic injection, voltage droop, flat-topping at the AC mains, that lead to poor power quality [88]. OBCs with high power levels, such AC Level 2 (>19.2 kW) and Level 3 require three-phase operation because of the limited power that can be drawn from a single phase supply. The variations of boost or buck type PFCs is discussed in detail in [89]. Since this paper focuses on high-voltage charging, this discussion is limited to three-phase boost-type PFCs for the sake of brevity. As seen in Table 7, BEV applications in North America require support of a three-phase PFC capable of managing 208-600 V_{LL}, since the three-phase distribution voltage levels in the

TABLE 7. OBC Voltage Range Based on Region and Charging Level

Region	1 Φ Voltage Range (V)	L1	L2	L3	3 Φ Voltage Range (V)	L1	L2	L3
North America	120-240	✓	✓		208-600			✓
Europe	230		✓		400		✓	✓
China	220		✓		380		✓	✓

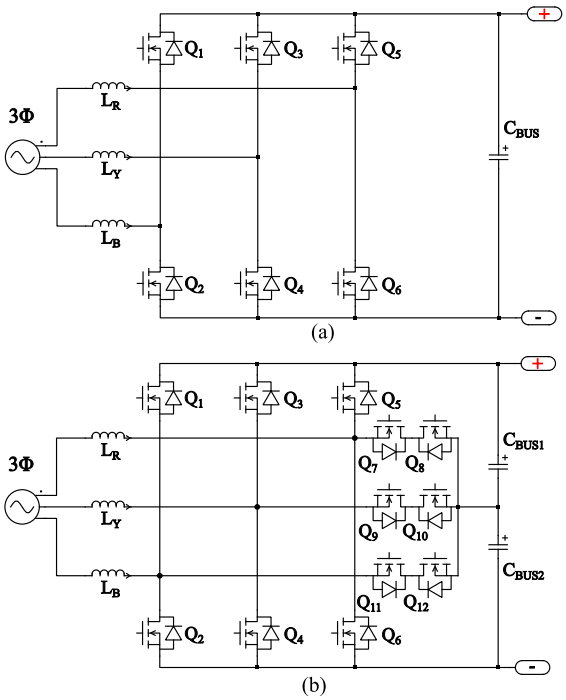

FIGURE 3. Three-phase full-bridge and 3L T-type PFC converters.

U.S. and Canada vary as 208Y/120, 480Y/277, 600Y/347, and are also under the purview of SAE J3068 [78]. It is also seen that Europe and China have one three-phase distribution voltage level at 400Y/230 V and 380Y/220 V respectively.

The three-phase full-bridge (FB) PFC is shown in Fig. 3(a). It is constructed using three inductors at the input of the bridge that act as the boost inductors, six active switches (Q_1 to Q_6), and a filter capacitor to develop the DC link. A 98.8% efficient Silicon Carbide (SiC) based 5 kW three-phase full-bridge PFC is developed in [90]. The three-phase three-level (3 L) T-type PFC is shown in Fig. 3(b). It is a boost type PFC constructed in the same philosophy as that of the full-bridge PFC, however it has six additional switches ($Q_7 - Q_{12}$) connected to the netural point generated by a split-capacitor network on the DC link. The additional switches are used to develop a 3-level waveform that provides a reduced dv/dt and better control on the boost inductor current, resulting in improved electromagnetic interference (EMI) and total harmonic distortion (THD) performances of the PFC stage [91]. A 97.3% efficient SiC based 10 kW three-phase T-type PFC is developed in [92]. Due to the high power operation of three-phase PFC rectifiers, they typically operate in the continuous conduction mode (CCM) [93]. Operation in

TABLE 8. Summary of Power Factor Correction (PFC) Stage Options

Topology	HV FETs	LV FETs	Diodes	Drivers	Voltage Sensors	Power	Switches	V_{dc}	f_{sw}	Eff.	Ref.
2L Full-Bridge	6	0	0	6	4	5 kW	SiC	700 V	45 kHz	98.8%	[90]
3L T-type	6	6	0	9	5	10 kW	SiC	800 V	50 kHz	97.3%	[92]
3L NPC	12	0	6	12	5	2 kW	IGBT	460 V	25 kHz	95.2%	[96]
3L ANPC	12	6	0	18	5	11 kW	GaN	800 V	100 kHz	98.2%	[98]
						4.2 kW	Si+SiC	650 V	40 kHz	99.1%	[100]
						10 kW	Si+SiC	570 V	140 kHz	99%	[101]

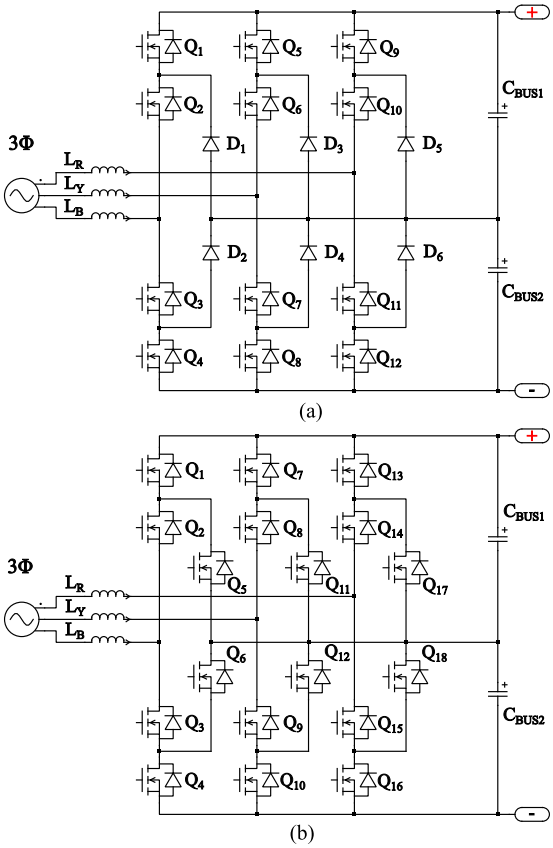

FIGURE 4. 3L NPC and 3L ANPC PFC converters.

CCM causes increased switching losses in the PFC rectifier and reduces its efficiency [94], [95]. The previously discussed PFC converters suffer with increased switching losses, that can be reduced using a neutral-point clamped (NPC) converter structure. Fig. 4(a) shows the schematic of a 3 L NPC PFC converter. It is constructed using three boost inductors, 12 switches ($Q_1 - Q_{12}$), six clamping diodes ($D_1 - D_6$) and a split DC bus using two capacitors. The 3 L NPC PFC suffers from doubled conduction losses since two additional switches are included in every current conduction path [58]. An IGBT based 95.2% efficient NPC converter has been developed for EV charging station applications in [96]. The efficiency of this converter is low, due to the use of Si IGBTs, and can be further improved with the use of SiC MOSFETs [97]. To reduce the forward conduction losses in the diode, they can be replaced by active clamps, resulting in further improved efficiency with the implication of increased cost. A 98.5% efficient 11 kW Gallium Nitride (GaN) based 3L-ANPC PFC stage has been developed by the authors in [98]. It is worth mentioning that an additional leg is required for balancing the capacitor voltage of a three-level converter in case the applied modulation scheme cannot maintain balance [99].

Table 8 shows the tabulated count of HV field effect transistors (FETs), low-voltage (LV) FETs, diodes, gate drivers, and voltage sensors required to construct the discussed topologies. The data on existing work is available for varying frequencies, voltages, and device technologies. Identifying the most viable trade-off as an option for the PFC stage requires an extensive common-baseline comparison curated for this application.

B. BIDIRECTIONAL ISOLATED DC-DC CONVERTER

The isolated DC-DC converter is encountered after the PFC stage, and is the link between the battery and DC link of the PFC stage. Galvanic isolation between the battery pack and the grid is a requirement of the UL 2202 standard, and is the conventional form of developing the DC-DC converter [102]. The risk of a shock during the converter operation is also governed by the leakage current limits between the battery's negative terminal and the vehicle chassis. There are some advances in transformerless DC-DC converters, by forcing the common-mode voltage to zero and eventually reducing leakage current to earth [103]. However, they are susceptible to unsafe operation due to single-point faults in the power converters that can risk exposure of a direct connection between the grid and battery pack. Systematic failure analysis and counter-measures against the identified failures is required to make it viable for mass adoption. The most commonly used isolated DC-DC converter topologies such as the two-level (2 L) dual active bridge (DAB), LLC, CLLC converter have been covered extensively in literature. The objective of this subsection is to focus on multi-level DC-DC converters that can be applied to the next-generation 800 V, 1.25 kV, and 1.5 kV classes of vehicles, a summary of which is shown in Table 9. Fig. 5 shows a LCL-T resonant network based stacked half-bridge (SHB) converter, which was proposed in [104]. This converter is fed from a constant voltage 800 V universal PFC output, and is intended for use in universal DC fast charging (150–950 V) with the means of external reconfiguration contactors. The mode created using a stacked half-bridge can be utilized for HV on-board charging applications. This converter is constructed using eight GaN high electron mobility transistors (HEMTs) ($Q_1 - Q_8$), an LCL-T

TABLE 9. Summary of Suitable DC-DC Converter Candidates for High-Voltage On-Board Charging

Bridge 1	Bridge 2	V_{in}	V_{out}	Power	f_{sw}	Eff.	Switches	Power Density	Ref.
3L SHB	3L SHB	800 V	750 V	6.60 kW	500 kHz	97.4%	GaN	7.3 kW/L	[104]
2L FB	3L NPC HB	750 V	1.7 - 2 kV	6.25 kW	100 kHz	97% *	SiC JFET	-	[105]
2L FB	3L NPC FB	292	1.68 kV	3.34 kW	5 kHz	88% †	IGBT	-	[108]
3L NPC FB	3L NPC FB	700 V	200 - 700 V	3.5 kW	50 kHz	95.5%	SiC	-	[109]
3 Φ FB	3 Φ NPC FB	400 V	1500 V	5 kW	50 kHz	-	SiC	-	[110]

* Modeled efficiency data, † 93% efficient transformer

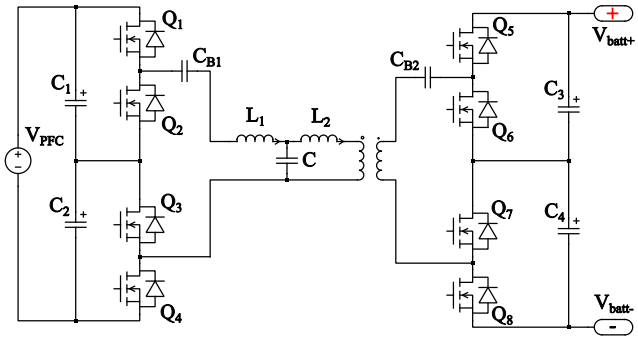

FIGURE 5. LCL-T network based stacked half-bridge converter [104].

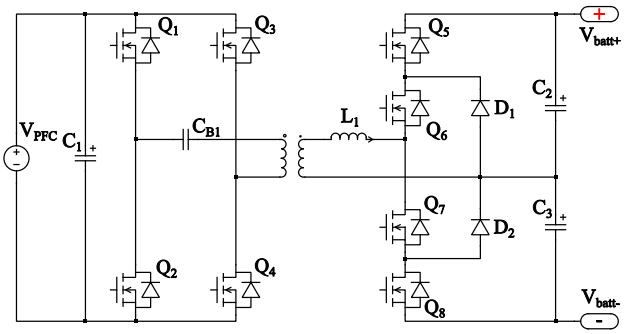

FIGURE 6. 2L FB - 3L NPC HB dual active bridge converter [105].

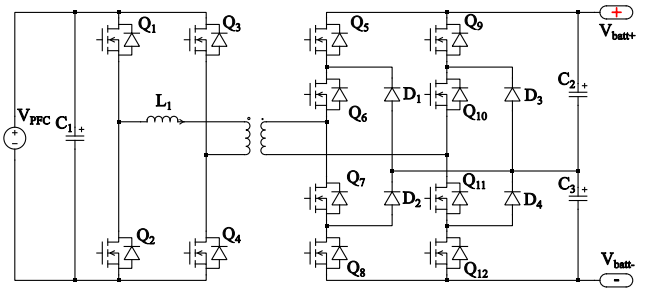

FIGURE 7. Multilevel dual active bridge converter [107].

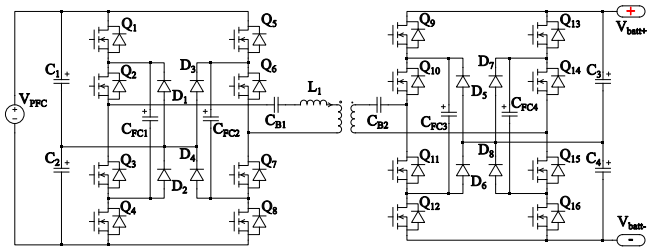

FIGURE 8. 3L dual active bridge converter with blocking capacitors [109].

network designed with a resonant frequency equal to the converter's switching frequency, and two DC blocking capacitors C_{B1} and C_{B2} to avoid transformer core saturation. This 6.6 kW converter exhibits a full-load efficiency of 97.4% at a battery voltage of 750 V.

Fig. 6 shows a dual active bridge converter constructed using a 2 L full-bridge (Q_1-Q_4), and isolation transformer, leakage inductance (L_1), and 3 L NPC half-bridge (HB) using (Q_5-Q_8, D_1, D_2) on the HV side, and is proposed in [105]. The intended use of this converter is in weight-sensitive aircraft applications with an 8 kV bus created using 4 serialized converters [106]. The output voltage of each converter is approximately 1.7–2 kV, and is thus useful in the HV on-board charging application as well. It is constructed using cascode-connected 1.7 kV SiC JFETs, operated at 100 kHz, and has an efficiency of 97%. Fig. 7 shows a multilevel dual active bridge converter constructed using a 2 L full-bridge on the LV side (Q_1-Q_4), a leakage inductance (L_1), isolation transformer, and a full-bridge constructed using 3 L NPC converters (Q_5-Q_{12}, D_1-D_4). This converter was first proposed by Moonem et al. for solar photovoltaic and DC microgrid applications in [107]. This converter is realized using IGBTs operated at 5 kHz, and exhibits a full load efficiency of 88%, while the transformer efficiency is at 93% [108]. Fig. 8 shows a 3 L dual active bridge converter with blocking capacitors [109]. It is an extension of the previously discussed multilevel dual active bridge converter, with a 3 L NPC bridge on both the interfaces, and DC blocking capacitors (C_{B1}, C_{B2}) to prohibit DC voltage generated by the 3 L NPC bridges to be passed to the transformer. An SiC based 3.5 kW DC-DC converter operating at 50 kHz exhibits a full-load efficiency of 95.5% at 700 V. Fig. 9 shows a 2L-3 L three-phase dual active bridge converter (DAB3) for solid-state transformers (SST) applications [110]. It is constructed using a three-phase 2 L

TABLE 10. Summary of Reference Designs and Commercialized On-Board Charger Sub-Systems

Converter	Maturity	Manufacturer	Power (kW)	Efficiency	AC Voltage	DC Voltage	Power Density	Reference
DC-DC	Ref. Design	Wolfspeed	22	98.5%	N/A	480-800	8 kW/L	[114]
DC-DC	Ref. Design	Infineon	11	97.2%	N/A	550-800	4.1 kW/L	[113]
AFE	Ref. Design	Wolfspeed	22	98.5%	305-450 V_{LL}	650-900	4.6 kW/L	[111]
AFE	Ref. Design	Wolfspeed	22	-	400-480 V_{LL}	800-900	-	[112]
OBC	Ref. Design	Infineon ETH Zürich	10	-	320-530 V_{LL}	250-1000	10 kW/L	[115]
OBC	Commercial	innoelectric	22	94%	380-480 V_{LL}	400-900	-	[116]
OBC	Commercial	EDN	22	94%	400-480 V_{LL}	up to 840	-	[117]

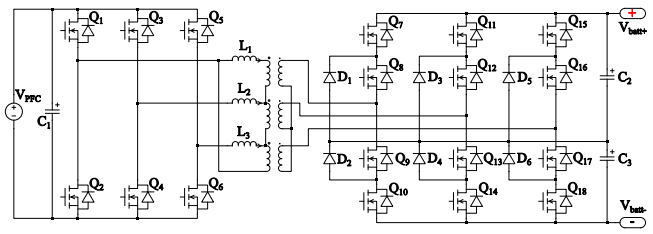

FIGURE 9. 2L-3L three-phase dual active bridge (DAB3) [110].

bridge (Q_1-Q_6), three single-phase high-frequency transformers connected in a Δ-Y configuration, leakage inductance, and a three-phase 3 L bridge on the high-voltage side. It has been tested for operation from 400 V to 1.5 kV, which makes it suitable for the HV on-board charger application. Efficiency data has not been reported for this configuration, however since the converter has a three-phase operation, it is suitable in building higher power building blocks of an on-board charger compared to all previously discussed topologies.

C. DEPLOYMENT CAPABLE DESIGNS

Table 10 shows the summary of commercial examples of either the sub-systems or the on-board charger. The current work does not cater to a battery voltage $>$ 1 kV, and is limited up to approximately 800 V, and opportunities for commercialization are present. Wolfspeed has developed a 98.5% efficient 22 kW SiC based PFC stage at a 4.6 kW/L power density [111]. Wolfspeed has presented the concept of a SiC based 25 kW PFC stage [112]. Infineon has developed a 97.2% efficient CLLC resonant DC-DC converter for an 800 V class vehicle's on-board charger with a 4.1 kW/L power density [113]. Wolfspeed has developed a 98.5% efficient CLLC resonant DC-DC converter with a 8 kW/L power density [114]. Infineon and ETH Zürich have co-developed a GaN based OBC demonstrator, based on a vienna rectifier PFC and series-parallel dual-active bridge DC-DC conversion stage [115]. EDN and innoelectric have commercialized 800 V class vehicles compatible on-board chargers [116], [117]. It is observed that the commercialized on-board chargers have poor efficiencies compared to a combination of AC-DC and DC-DC converter's reference design efficiency, which can be attributed to need of slowing down the switching operation at the cost of EMI reduction for qualification of regulatory standards for commercialization.

TABLE 11. Summary of Regulatory Standards Applicable to On-Board Charger Development

Standard	Description
IEEE 519 IEC 61000-3-2*	Limits of the harmonics injected into the grid from the EVSE
CISPR 25	Limits of radiated/conducted electromagnetic interference
ISO 11542	Test of the OBC's susceptibility to radiated /conducted electromagnetic interference
ISO 10605	Electrostatic discharge (ESD) susceptibility
ISO 16750	Environmental Stress for ESAs
ISO 26262	Development cycle recommendation for functional safety assessment and design
UL 2202	Electrical safety test for an on-board charger
ISO 15118	Vehicle to grid (V2G) operation's communication interface specifications

* Applicable in Europe [89]

D. REGULATORY STANDARDS

Since the on-board charger is an electronic sub-assembly (ESA), it is required to comply with certain regulatory standards for safe vehicle operation, interoperability and acceptance to be integrated in the vehicle. Table 11 shows a summary of the standards required to be complied in case of the development of an on-board charger. IEEE 519 and IEC 61000-3-2 are power quality regulations to determine the total harmonic distortion (THD) limits beyond which it is forbidden to operate a power converter at a point of common coupling (PCC), which in the context of on-board chargers is an EVSE [89], [118]. CISPR 25, segregated as Class 1 (most lenient) to Class 5 (most stringent) governs the limits of conducted and radiated EMI during the operation of the on-board

charger [119]. The scope of the CISPR 25 standard is limited for voltages up to 1 kV, and hence requires re-assessment to be applied for the the 1–1.5 kV battery voltage range. To verify the susceptibility of the on-board charger's operation under external EMI imposed on it, ISO 11452-1 to ISO 11452-11 covers the tests related to electromagnetic susceptibility, such as bulk current injection (BCI) and absorber-lined shielded enclosure (ALSE) methods [120], [121]. ISO 10605 describes the test procedures to evaluate the immunity of a module against electrostatic discharge (ESD) [122]. The environmental stresses such as thermal, humidity, vibration tests are defined by ISO 16750. To reduce the risk of systematic faults in the vehicle, a functional safety compliant development cycle can be utilized if the on-board charger is deemed to be safety-critical in nature based on the system's safety failure mode effects and analysis (S-FMEA) [54]. UL 2202 defines the electrical safety requirements of on-board battery chargers, and the subjected tests are in the category of leakage current, operational safety, vibration, and environmental stress [102]. ISO 15118 defines the requirements of vehicle to grid (V2G) communication for bidirectional discharging/charging of electric vehicles, determines the details of the application protocols requirements for interoperability [123].

VI. ON-BOARD CHARGER INTEGRATION

The U.S. DRIVE program has set efficiency, power density, and cost targets for the sub-systems in an electric vehicle powertrain to enable faster adoption of BEVs [124]. This requires OEMs to focus on eliminating redundant ESAs, and further optimize integration within the powertrain. This Section discusses studies performed for single-stage on-board chargers, traction-integrated on-board chargers, and APU integrated on-board chargers.

A. PFC AND ISOLATED DC-DC CONVERTER STAGE INTEGRATION

In a typical on-board charger, the first stage is the AC-DC conversion stage, followed by the isolated DC-DC converter stage for developing the link between the grid and the high-voltage battery pack. The switch count can be reduced and the DC link capacitor can be eliminated by combining the AC-DC and DC-DC stages. A matrix converter based isolated three-phase bidirectional on-board charger has been proposed in [125]. It utilizes a higher switch count compared to a conventional two-stage approach. However, the DC link electrolytic capacitor is eliminated, resulting in higher reliability. A single-phase isolated totem-pole ZVS converter for bidirectional on-board charging, with a peak efficiency of 96.7% in the G2V mode, and 96.2% in the V2G mode is proposed in [126]. This work is also further extended to both single-phase and three-phase operation in [127]. The peak efficiency of the 11 kW on-board charger with a power density of 4.15 kW/L is 97.01%. It is worth noting that, a comparison of DAB based single-stage and two-stage topologies concludes that the integrated totem-pole DAB encompasses 23% higher volume than a DAB with dual-phase shift (DPS) modulation [128].

B. PFC AND AUXILIARY POWER UNIT INTEGRATION

The on-board charger has a high-voltage bridge that interacts with the high-voltage battery pack for modulating the power flow to it. The APU also contains a high-voltage bridge, capable of modulating power to the low-voltage battery via an isolation transformer. Due to a common interface at the high-voltage battery pack, there is an opportunity to reduce the system-level switch count. This is achievable by incorporating a multiport transformer between the PFC output, high-voltage battery, and the low-voltage battery. Multiport converters have been heavily utilized in the solar and energy storage industries [129]. A 94% efficient CLLC resonant converter based dual output converter for 400 V BEV integration with a 12 V APU, utilizing frequency control has been proposed in [130]. A phase-shift control based 500 W series resonant three port converter for energy storage applications has been proposed in [131]. Its application can be further extended for a PFC integrated APU.

C. TRACTION INVERTER INTEGRATION

In a BEV powertrain, the traction inverter has the highest power handling capability (typically $>$ 100 kW) among all power electronics components. As the power rating of AC Level 3 on board charging has the capability to reach up to 166 kW, it is redundant to have another set of power electronic components to manage interaction of power flow between the grid and the high-voltage battery pack. A review of traction inverter integrated on-board chargers has been done in [132]. The objective across multiple implementation methodologies has been to route the three-phase AC inlet to the propulsion motor, reconfigure the propulsion motor to use its self-inductance as a boost inductor, and use the traction inverter a boost rectifier stage. The two main challenges in this methodology are to ensure that no torque is generated on the propulsion motor when charging is enabled and the safety risk to the user due to lack of galvanic isolation between the high-voltage battery and grid, that have made commercial adoption challenging. A six-phase machine based isolated integrated on-board charger is proposed in [133]. Achieving three-phase isolation with a three-phase propulsion motor is not possible, hence a multi-phase traction inverter would be required to develop a three-phase isolated integrated charger. It is worth mentioning that multi-phase traction inverters have some disadvantages in high-voltage applications [134]. A holistic system-level evaluation of the required power, voltage, efficiency, and cost of an integrated MHDV powertrain contextualized to its application scenario can be evaluated for a high-voltage multi-phase propulsion system.

To maintain isolation between the high-voltage battery and the grid, another method is to primarily rely on an external DC fast charging infrastructure and reconfigure the traction

TABLE 12. Required Standoff Voltages Based on Number of Levels

DC fast charging standard	Max. Voltage (V)	Required Standoff Voltage (V)		
		2L	3L	5L
ChaoJi/ CHAdeMO 3.0	1500	1950	975	488
Megawatt Charging System (MCS)	1250	1625	813	407

inverter as a boost rectifier for performing CC-CV charging [135]. This is particularly useful for backward integration of DC fast chargers with a low-voltage output compared to the battery pack voltage, without compromising the charging speed and the necessity to add extra power electronics to match voltage levels.

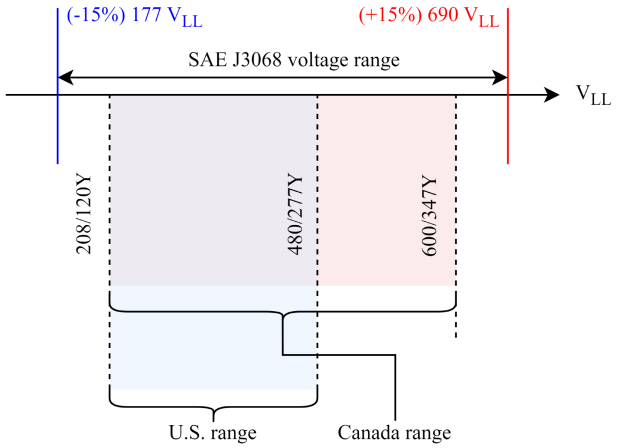

FIGURE 10. Three-phase voltage ranges in U.S. and Canada.

VII. FUTURE CHALLENGES

This Section discusses the current gaps in technology to aid the development of performance focused and commercially viable high-voltage compatible on-board chargers while defining the of concern that need to be addressed. Challenges related to the readiness of automotive qualified semiconductors, wide three-phase operation in North America, and integration of conductive and wireless charging are discussed.

A. AUTOMOTIVE QUALIFIED HV SEMICONDUCTORS

Table 12 shows the required semiconductor standoff voltage as a function of the maximum battery voltage and the number of levels of operation, assuming a 30% voltage derating. Since the on-board charger is an EV sub-system exposed to harsh vibrations, thermal stress, and varying humidity. AEC-Q101 certification of semiconductors is required to pass the reliability qualification requirements and reduce failure rates of deployed sub-systems [136]. In the context of SiC devices, major manufacturers supply devices rated at 650 V, 750 V, 900 V, 1 kV, 1.2 kV, and 1.7 kV [137], [138], [139]. Infineon and GeneSiC are the only manufacturers that support 2 kV and 3.3 kV SiC MOSFETs [140], [141]. SiC MOSFETs with standoff voltages up to 15 kV are available, however their maturity is limited to industrial applications. For 2-level operation of the DC-DC converter, focused development of a device class in the 2 kV range would be beneficial for mass adoption, since use of the 3.3 kV device class would provide an over designed safety margin for the said voltage levels. No manufacturers currently support AEC-Q101 qualified devices in the $>$ 1.2 kV device class, and further qualification is required in this segment. 3-level operation can be supported with existing devices.

Since the 1.7 kV device class is a viable candidate for MCS compliant on-board chargers, a comparison is performed based on state-of-the-art devices, and the viability of choosing between 2 or 3-level operation. Table 13 shows a comparison of 1.7 kV and 1.2 kV rated devices. Since zero voltage switching (ZVS) is easily possible in resonant converters, turn-on energies have been neglected for brevity. $E_{off(1700)}$ and $E_{off(1200)}$ are the turn-off energies, whereas $R_{ds(on),1700}$ and $R_{ds(on),1200}$ are the on-state resistances of the devices. $P_{loss,adv}$ is a metric that shows the advantage offered by using 1.2 kV devices in a 3-level operation, as compared to 1.7 kV devices in a 2-level operation for a 50% switching and conduction loss distribution, as seen in (2). The cost of constructing an M-level NPC bridge C_{ML}, where M is the number of voltage levels, C_{MOS}, C_{drv}, C_{PS}, C_D are the cost of the MOSFET, gate driver, gate driver power supply and clamping diodes quoted at 10,000 units, as seen in (3) [142].

$$P_{loss,adv} = 1 - \frac{1}{2}\left(\frac{2.E_{off,1200}}{E_{off,1700}} + \frac{R_{ds(on),1200}}{R_{ds(on),1700}}\right) \quad (2)$$

$$C_{ML} = 4(M-1)(C_{MOS}+C_{drv}+C_{PS})+4(M-2)C_D \quad (3)$$

Table 13 shows a normalized power loss and cost comparison of choosing to construct a 1.25 kV compatible full-bridge using a 2-level or 3-level NPC converter. On an average, the 3-level converter based option provides about 31% advantage in the total power losses. Despite the addition of added gate drivers and clamping diodes, the 3-level NPC based option costs about -20% lower. This also highlights the disparity in the switching energy and cost that needs to be addressed by SiC semiconductor manufacturers for OEMs to choose between 2-level and 3-level operation.

GaN HEMTs aid in increasing the converter's operating frequency, and thus reduce the size of the magnetics. Production GaN HEMTs are available at a maximum voltage of 900 V. Hence in this case, a 3-level operation is not supported only in the MCS case, while a ChaoJi compliant GaN based solution requires 5-level operation.

B. WIDE THREE-PHASE VOLTAGE IN NORTH AMERICA

As shown in Fig. 10, in the U.S., 208/120Y and 480/277Y are the common three-phase voltages, while in Canada, 208/120Y and 600/347Y are the common voltages for three-phase LV distribution [143]. Due to shared land borders and economic

TABLE 13. Cost and Normalized Loss Comparison of a 2 L and 3 L Converter Based Bridge for a 1.25 kV On-Board Charger

Manufacturer	1700 V Part	$R_{ds,1700}$	$E_{off,1700}$	1200 V Part	$R_{ds,1200}$	$E_{off,1200}$	$P_{loss,adv}$	C_{2L}	C_{3L}
GeneSiC	G3R20MT17K	20 $m\Omega$	300 μJ at V_{ds} = 1.2 kV I_{ds} = 30 A	G3R20MT12K	20 $m\Omega$	50 μJ at V_{ds} = 600 V I_{ds} = 30 A	33%	$433	$377
Wolfspeed	C2M0045170P	45 $m\Omega$	220 μJ at V_{ds} = 1.2 kV I_{ds} = 30 A	C3M0040120K	40 $m\Omega$	60 μJ at V_{ds} = 600 V I_{ds} = 30 A	28%	$364	$268

co-dependency between the U.S. and Canada, $828 billion of North American transborder freight was accounted in the year 2021 [144]. Due to this reason, the on-board charger of a medium and heavy-duty vehicle operating in North America is required to support voltages from 208-600 V_{LL}, as shown in Table 7. The minimum line-line voltage is 208 V_{LL}, while the maximum line-line voltage is 600 V_{LL}. SAE J3068 requires the on-board charger to accept ±15% voltage sag or swell on its input voltage capability communicated to the EVSE [78]. This results in a required input voltage range of 177-690 V_{LL}, and the on-board charger must be designed to operate efficiently throughout this voltage range. A 10 kW variable turns ratio semi-DAB converter with a peak efficiency of 98.5% is proposed for DC fast charging applications [145]. The proposed converter is unidirectional, and this work can be extended to a bidirectional use case for wide PFC voltage operation. A reconfiguration mechanism for a partially-paralleled DAB converter (P^2DAB) to improve the charging efficiency for a wide-output (200 V–1 kV) DC fast charger has been proposed in [146]. The proposed converter is bidirectional in nature, and can be adopted for wide PFC voltage operation.

C. INTEGRATION WITH WIRELESS CHARGING

SAE J2954 is a standard developed for wireless power transfer (WPT) of power levels up to 3.3 kW, 7.7 kW, 11 kW, and 22 kW [147]. The standard mandates that vehicles compliant with SAE J2954 should also support conductive charging via SAE J1772. Recently, SAE has released an initial specification of SAE TIR J2954/2, which defines higher power levels up to 500 kW for both dynamic and static WPT of medium and heavy-duty electric vehicles [148]. This standard is an initial release, and does not recommend OEMs to comply to it as of now. Further updates to this version requires considering the voltage level compatibility with MCS and ChaoJi/ CHAdeMO 3.0. System integration of co-dependency considering wireless charging and on-board charging for high-voltage powertrain applications has significant research potential.

VIII. CONCLUSION

The automotive sector is witnessing an increase in the sale of electrified vehicles. Governments all over the world are investing heavily for the deployment of charging infrastructure in order to further increase the adoption of cleaner vehicles with a reduced carbon dioxide equivalent (CO_2Eq.) footprint. State-of-the-art DC fast charging times are almost eight times longer than the refuelling time required for conventional gasoline-powered vehicles and thus, act as a deterrent to the adoption of electrified vehicles. Increasing the DC fast charging power is a solution to reduce the charging time, and is aided by the introduction of new high-voltage DC fast charging standards. Electrification of medium and heavy duty vehicles is also gaining traction, which could benefit from high-voltage powertrains. The co-dependency of DC fast charging and on-board charging for high-voltage powertrains is studied to build a case regarding the upcoming technical challenges and implications on high-voltage on-board charging. Since existing power converter topologies are based on state-of-the-art semiconductors, with limited voltage ratings not currently suitable for high-voltage systems, investigation of multilevel converters becomes necessary. The recent advances in integrated on-board charging have been summarized. The gaps in state-of-the-art technology and roadblocks in developing the next-generation of high-voltage on-board chargers are summarized to establish the direction of further research areas in semiconductors, wide-voltage range power converters, and system-level integration of conductive and wireless charging.

REFERENCES

[1] D. L. Bleviss, "Transportation is critical to reducing greenhouse gas emissions in the United States," *Wiley Interdiscipl. Rev.: Energy Environ.*, vol. 10, no. 2, 2021, Art. no. e390.

[2] B. Bilgin et al., "Making the case for electrified transportation," *IEEE Trans. Transport. Electrific.*, vol. 1, no. 1, pp. 4–17, Jun. 2015.

[3] J. Buberger, A. Kersten, M. Kuder, R. Eckerle, T. Weyh, and T. Thiringer, "Total CO2-equivalent life-cycle emissions from commercially available passenger cars," *Renew. Sustain. Energy Rev.*, vol. 159, 2022, Art. no. 112158.

[4] I. Aghabali, J. Bauman, P. J. Kollmeyer, Y. Wang, B. Bilgin, and A. Emadi, "800-V electric vehicle powertrains: Review and analysis of benefits, challenges, and future trends," *IEEE Trans. Transport. Electrific.*, vol. 7, no. 3, pp. 927–948, Sep. 2021.

[5] O. Elma, "A dynamic charging strategy with hybrid fast charging station for electric vehicles," *Energy*, vol. 202, 2020, Art. no. 117680.

[6] International Copper Association, "The electric vehicle market and copper demand," 2017. [Online]. Available: https://copperalliance.org/wp-content/uploads/2017/06/2017.06-E-Mobility-Factsheet-1.pdf

[7] L. Wang, Z. Qin, T. Slangen, P. Bauer, and T. van Wijk, "Grid impact of electric vehicle fast charging stations: Trends, standards, issues and mitigation measures - An overview," *IEEE Open J. Power Electron.*, vol. 2, pp. 56–74, 2021.

[8] G. H. Broadbent, G. Metternicht, and D. Drozdzewski, "An analysis of consumer incentives in support of electric vehicle uptake: An Australian case study," *World Electric Veh. J.*, vol. 10, no. 1, 2019, Art. no. 11.

[9] A. Khaligh and S. Dusmez, "Comprehensive topological analysis of conductive and inductive charging solutions for plug-in electric vehicles," *IEEE Trans. Veh. Technol.*, vol. 61, no. 8, pp. 3475–3489, Oct. 2012.

[10] A. Khaligh and M. D'Antonio, "Global trends in high-power on-board chargers for electric vehicles," *IEEE Trans. Veh. Technol.*, vol. 68, no. 4, pp. 3306–3324, Apr. 2019.

[11] J. Yuan, L. Dorn-Gomba, A. D. Callegaro, J. Reimers, and A. Emadi, "A review of bidirectional on-board chargers for electric vehicles," *IEEE Access*, vol. 9, pp. 51501–51518, 2021.

[12] H. Tu, H. Feng, S. Srdic, and S. Lukic, "Extreme fast charging of electric vehicles: A technology overview," *IEEE Trans. Transport. Electrific.*, vol. 5, no. 4, pp. 861–878, Dec. 2019.

[13] International Energy Agency, "Global electric vehicle outlook 2022," 2022. [Online]. Available: https://www.iea.org/reports/global-ev-outlook-2022

[14] M. Etezadi-Amoli, K. Choma, and J. Stefani, "Rapid-charge electric-vehicle stations," *IEEE Trans. Power Del.*, vol. 25, no. 3, pp. 1883–1887, Jul. 2010.

[15] T. R. Tanim, M. G. Shirk, R. L. Bewley, E. J. Dufek, and B. Y. Liaw, "Fast charge implications: Pack and cell analysis and comparison," *J. Power Sources*, vol. 381, pp. 56–65, 2018.

[16] M. Yilmaz and P. T. Krein, "Review of battery charger topologies, charging power levels, and infrastructure for plug-in electric and hybrid vehicles," *IEEE Trans. Power Electron.*, vol. 28, no. 5, pp. 2151–2169, May 2013.

[17] M. Shirk and J. Wishart, "Effects of electric vehicle fast charging on battery life and vehicle performance," Idaho Nat. Lab., Idaho Falls, ID, USA, Tech. Rep., INL/CON-14-33490, 2015.

[18] M. Hoshi, "Electric vehicles and expectations for wide bandgap power devices," in *Proc. IEEE 28th Int. Symp. Power Semicond. Devices ICs*, 2016, pp. 5–8.

[19] C. Panchal, S. Stegen, and J. Lu, "Review of static and dynamic wireless electric vehicle charging system," *Eng. Sci. Technol., Int. J.*, vol. 21, no. 5, pp. 922–937, 2018.

[20] A. Ahmad, M. S. Alam, and R. Chabaan, "A comprehensive review of wireless charging technologies for electric vehicles," *IEEE Trans. Transport. Electrific.*, vol. 4, no. 1, pp. 38–63, Mar. 2018.

[21] International Energy Agency, "Trends in charging infrastructure," 2022. [Online]. Available: https://www.iea.org/reports/global-ev-outlook-2022/trends-in-charging-infrastructure

[22] C. Dharmakeerthi, N. Mithulananthan, and T. Saha, "Impact of electric vehicle fast charging on power system voltage stability," *Int. J. Elect. Power Energy Syst.*, vol. 57, pp. 241–249, 2014.

[23] K. Qian, C. Zhou, and Y. Yuan, "Impacts of high penetration level of fully electric vehicles charging loads on the thermal ageing of power transformers," *Int. J. Elect. Power Energy Syst.*, vol. 65, pp. 102–112, 2015.

[24] H. Zhang, Z. Hu, Z. Xu, and Y. Song, "An integrated planning framework for different types of PEV charging facilities in urban area," *IEEE Trans. Smart Grid*, vol. 7, no. 5, pp. 2273–2284, Sep. 2016.

[25] A. G. Boulanger, A. C. Chu, S. Maxx, and D. L. Waltz, "Vehicle electrification: Status and issues," *Proc. IEEE*, vol. 99, no. 6, pp. 1116–1138, Jun. 2011.

[26] ChargeHub, "Guide on how to charge your electric car with charging stations," 2022. [Online]. Available: https://chargehub.com/en/electric-car-charging-guide.html

[27] P. Morrissey, P. Weldon, and M. O'Mahony, "Future standard and fast charging infrastructure planning: An analysis of electric vehicle charging behaviour," *Energy Policy*, vol. 89, pp. 257–270, 2016.

[28] Lucid Motors, "Battery pack tech talks," 2022. [Online]. Available: https://www.youtube.com/watch?v=2aDyjJ5wj64

[29] Lucid Motors, "Lucid air specs," 2021. [Online]. Available: https://www.lucidmotors.com/air/specs

[30] A. Nedelea, "Lucid air touring won't be available until q4 2022," INSIDEEVs, 2022. [Online]. Available: https://insideevs.com/news/587888/lucid-air-touring-available-q4-2022/

[31] Audi MediaCenter, "Battery and thermal management," 2021. [Online]. Available: https://www.audi-mediacenter.com/en/emotive-design-and-revolutionary-technologythe-audi-e-tron-gt-quattro-and-the-audi-rs-e-tron-gt-13655/battery-and-thermal-management-13784

[32] Audi MediaCenter, "Audi further improves the e-tron product line: Ac charging with 22 kW of power, greater driving convenience," 2020. [Online]. Available: https://www.audi-mediacenter.com/en/press-releases/audi-further-improves-the-e-tron-product-lineac-charging-with-22-kw-of-power-greater-driving-convenience-13361

[33] BYD, "Byd's new blade battery set to redefine EV safety standards," 2020. [Online]. Available: https://en.byd.com/news/byds-new-blade-battery-set-to-redefine-ev-safety-standards

[34] BYD, "Byd han EV specifications & configurations," 2020. [Online]. Available: https://quantumauto.com.do/wp-content/uploads/2021/07/Han-EV.pdf

[35] P. Newsroom, "Sophisticated thermal management, up to 800-volt system voltage," 2021. [Online]. Available: https://media.porsche.com/mediakit/taycan/en/porsche-taycan/die-batterie

[36] P. Newsroom, "Quick, comfortable, intelligent and universal," 2021. [Online]. Available: https://media.porsche.com/mediakit/taycan/en/porsche-taycan/das-laden

[37] F. Lambert, "Tesla confirms new 82 kwh battery pack in model 3, thanks to new cells," electrek, 2020. [Online]. Available: https://electrek.co/2020/11/10/tesla-model-3-82-kwh-battery-pack-new-cells/

[38] Tesla, "Support: Onboard charger," 2018. [Online]. Available: https://www.tesla.com/support/home-charging-installation/onboard-charger

[39] N. Nitta, F. Wu, J. T. Lee, and G. Yushin, "Li-ion battery materials: Present and future," *Mater. Today*, vol. 18, no. 5, pp. 252–264, 2015.

[40] C. Xu, Q. Dai, L. Gaines, M. Hu, A. Tukker, and B. Steubing, "Future material demand for automotive lithium-based batteries," *Commun. Mater.*, vol. 1, no. 1, pp. 2662–4443, 2020.

[41] T. Waldmann, R.-G. Scurtu, K. Richter, and M. Wohlfahrt-Mehrens, "18650 vs. 21700 li-ion cells–a direct comparison of electrochemical, thermal, and geometrical properties," *J. Power Sources*, vol. 472, 2020, Art. no. 228614.

[42] T. Liu, J. P. Vivek, E. W. Zhao, J. Lei, N. Garcia-Araez, and C. P. Grey, "Current challenges and routes forward for nonaqueous lithium–air batteries," *Chem. Rev.*, vol. 120, no. 14, pp. 6558–6625, 2020.

[43] J. Schnell et al., "All-solid-state lithium-ion and lithium metal batteries–paving the way to large-scale production," *J. Power Sources*, vol. 382, pp. 160–175, 2018.

[44] SAE, "SAE j1772-2001 SAE electric vehicle conductive charge coupler," 2001. [Online]. Available: https://www.sae.org/standards/content/j1772_200111/

[45] Tesla Blog, "We have begun regular production of the tesla roadster," 2008. [Online]. Available: https://www.tesla.com/blog/we-have-begun-regular-production-tesla-roadster

[46] T. Chen et al., "A review on electric vehicle charging infrastructure development in the UK," *J. Modern Power Syst. Clean Energy*, vol. 8, no. 2, pp. 193–205, 2020.

[47] U. S. Department of Transportation, "President biden, usdot and usdoe announce 5 billion over five years for national EV charging network, made possible by bipartisan infrastructure law," 2022. [Online]. Available: https://highways.dot.gov/newsroom/president-biden-usdot-and-usdoe-announce-5-billion-over-five-years-national-ev-charging

[48] S. Tetik, "Megawatt charging system (MCS)," CharIN, 2022. [Online]. Available: https://www.charin.global/technology/mcs/

[49] SAE, "Megawatt charging system for electric vehicles," 2021. [Online]. Available: https://www.sae.org/standards/content/j3271/

[50] SAE, "New chademo 3.0 aims to harmonize global EV quick-charging standards," 2020. [Online]. Available: https://www.sae.org/news/2020/05/chademo-3.0-to-harmonize-global-ev-quick-charging-standards

[51] M. Khalid, F. Ahmad, B. K. Panigrahi, and L. Al-Fagih, "A comprehensive review on advanced charging topologies and methodologies for electric vehicle battery," *J. Energy Storage*, vol. 53, 2022, Art. no. 105084.

[52] Underwriters Laboratories, "Ul 2580: Batteries for use in electric vehicles," 2022. [Online]. Available: https://www.shopulstandards.com/ProductDetail.aspx?productId=UL2580

[53] D. Marcos et al., "A safety concept for an automotive lithium-based battery management system," in *Proc. Electric Veh. Int. Conf.*, 2019, pp. 1–6.

[54] ISO, "ISO 26262-2:2018, road vehicles – functional safety – part 2: Management of functional safety," 2018. [Online]. Available: https://www.iso.org/standard/68384.html

[55] Texas Instruments, "AMC1411-Q1: Automotive, 2-V input, precision voltage sensing reinforced isolated amplifier with high CMTI," 2021. [Online]. Available: https://www.ti.com/product/AMC1411-Q1

[56] TE Connectivity, "High-voltage contactors: Safely connect and disconnect," [Online]. Available: https://www.te.com/usa-en/products/relays-contactors-switches/contactors/automotive-contactors.html

[57] A. Emadi, Y. J. Lee, and K. Rajashekara, "Power electronics and motor drives in electric, hybrid electric, and plug-in hybrid electric vehicles," *IEEE Trans. Ind. Electron.*, vol. 55, no. 6, pp. 2237–2245, Jun. 2008.

[58] M. Schweizer and J. W. Kolar, "Design and implementation of a highly efficient three-level t-type converter for low-voltage applications," *IEEE Trans. Power Electron.*, vol. 28, no. 2, pp. 899–907, Feb. 2013.

[59] L. Zhang et al., "Evaluation of different Si/SiC hybrid three-level active NPC inverters for high power density," *IEEE Trans. Power Electron.*, vol. 35, no. 8, pp. 8224–8236, Aug. 2020.

[60] A. Poorfakhraei, M. Narimani, and A. Emadi, "A review of multilevel inverter topologies in electric vehicles: Current status and future trends," *IEEE Open J. Power Electron.*, vol. 2, pp. 155–170, 2021.

[61] J. Reimers, L. Dorn-Gomba, C. Mak, and A. Emadi, "Automotive traction inverters: Current status and future trends," *IEEE Trans. Veh. Technol.*, vol. 68, no. 4, pp. 3337–3350, Apr. 2019.

[62] A. Poorfakhraei, M. Narimani, and A. Emadi, "Improving power density of a three-level ANPC structure using the electro-thermal model of inverter and a modified SPWM technique," *IEEE Open J. Power Electron.*, vol. 3, pp. 741–754, 2022.

[63] S. Halder, P. Agarwal, and S.P. Srivastava, "MTPA based sensorless control of PMSM using position and speed estimation by back-EMF method," in *Proc. IEEE 6th Int. Conf. Power Syst.*, 2016, pp. 1–4.

[64] T. A. Burress et al., "Evaluation of the 2010 toyota prius hybrid synergy drive system," 2011. [Online]. Available: https://www.osti.gov/biblio/1007833

[65] B. Kim, K. Kim, and S. Choi, "A 800V/14V soft-switched converter with low-voltage rating of switch for XEV applications," in *Proc. Int. Power Electron. Conf.*, 2018, pp. 256–260.

[66] A. Adler, "Exclusive first ride: Nikola electric truck can turn on a dime," *FreightWaves*, 2021. [Online]. Available: https://www.freightwaves.com/news/exclusive-first-ride-nikola-electric-truck-can-turn-on-a-dime

[67] Tesla, "Tesla semi," 2021. [Online]. Available: https://www.tesla.com/en_ca/semi

[68] BYD, "Byd k9 40' transit," 2022. [Online]. Available: https://en.byd.com/bus/k9m/

[69] BYD, "Byd k11 60' transit," 2022. [Online]. Available: https://en.byd.com/bus/k11 m/

[70] Scania, "Battery electric truck," 2022. [Online]. Available: https://www.scania.com/group/en/home/products-and-services/trucks/battery-electric-truck.html

[71] L. Saw, A. A. O. Tay, and L. W. Zhang, "Thermal management of lithium-ion battery pack with liquid cooling," in *Proc. 31st Thermal Meas., Model. Manage. Symp. (SEMI-THERM)*, 2015, pp. 298–302.

[72] M. Uitz et al., "Aging of Tesla's 18650 lithium-ion cells: Correlating solid-electrolyte-interphase evolution with fading in capacity and power," *J. Electrochem. Soc.*, vol. 164, no. 14, 2017, Art. no. A3503.

[73] G. Bauer, C.-W. Hsu, M. Nicholas, and N. Lutsey, "Charging up America: Assessing the growing need for U.S. charging infrastructure through 2030," *Int. Council Clean Transp.*, 2021, pp. 1–45.

[74] SAE, "SAE j1772-2017 SAE electric vehicle conductive charge coupler," 2017. [Online]. Available: https://www.sae.org/standards/content/j1772_201710/

[75] Tesla, "Tesla mobile connector." [Online]. Available: https://www.tesla.com/support/home-charging-installation/mobile-connector

[76] International Electrotechnical Commission, "IEC 62196-2:2016, plugs, socket-outlets, vehicle connectors and vehicle inlets - conductive charging of electric vehicles - Part 2: Dimensional compatibility and interchangeability requirements for A.C. pin and contact-tube accessories," 2016. [Online]. Available: https://webstore.iec.ch/publication/24204

[77] Standardization Administration of China, "Gb/t 20234.1-2015: Connection set for conductive charging of electric vehicles–Part 1: General requirements," 2015. [Online]. Available: http://webstore.spc.net.cn/produce/showonebook.asp?strid=76754

[78] SAE, "SAE j3068–2018 electric vehicle power transfer system using a three-phase capable coupler," 2018. [Online]. Available: https://www.sae.org/standards/content/j3068_201804

[79] Lucid Motors, "Charging and the wunderbox tech talks," 2022. [Online]. Available: https://www.youtube.com/watch?v=Ga0qMqUG2X4

[80] Vicor Power, "The challenge of range anxiety from DC fast-charging incompatibility," 2021. [Online]. Available: https://www.vicorpower.com/industries-and-innovations/automotive/dc-fast-charging

[81] M. A. H. Rafi and J. Bauman, "A comprehensive review of DC fast-charging stations with energy storage: Architectures, power converters, and analysis," *IEEE Trans. Transport. Electrific.*, vol. 7, no. 2, pp. 345–368, Jun. 2021.

[82] S. Srdic and S. Lukic, "Toward extreme fast charging: Challenges and opportunities in directly connecting to medium-voltage line," *IEEE Electrific. Mag.*, vol. 7, no. 1, pp. 22–31, Mar. 2019.

[83] SAE, "Sae j3105-2020 electric vehicle power transfer system using conductive automated connection devices," 2020. [Online]. Available: https://www.sae.org/standards/content/j3105_202001/

[84] T. Bohn and H. Glenn, "A real world technology testbed for electric vehicle smart charging systems and PEV-EVSE interoperability evaluation," in *Proc. IEEE Energy Convers. Congr. Expo.*, 2016, pp. 1–8.

[85] J. Parmar, P. Das, and S. M. Dave, "Study on demand and characteristics of parking system in urban areas: A review," *J. Traffic Transp. Eng. (English Edition)*, vol. 7, no. 1, pp. 111–124, 2020.

[86] F. Lambert, "Tesla spotted using mobile powerpacks at first tesla semi megacharger station," *electrek*, 2022. [Online]. Available: https://electrek.co/2022/01/10/tesla-spotted-mobile-powerpacks-first-tesla-semi-megacharger-station/

[87] S. Jaman et al., "Development and validation of V2G technology for electric vehicle chargers using combo CCS type 2 connector standards," *Energies*, vol. 15, no. 19, 2022, Art. no. 7364.

[88] B. Singh, B. Singh, A. Chandra, K. Al-Haddad, A. Pandey, and D. P. Kothari, "A review of three-phase improved power quality AC-DC converters," *IEEE Trans. Ind. Electron.*, vol. 51, no. 3, pp. 641–660, Jun. 2004.

[89] J. W. Kolar and T. Friedli, "The essence of three-phase PFC rectifier systems–Part I," *IEEE Trans. Power Electron.*, vol. 28, no. 1, pp. 176–198, Jan. 2013.

[90] A. Kouchaki and M. Nymand, "High efficiency three-phase power factor correction rectifier using sic switches," in *Proc. 19th Eur. Conf. Power Electron. Appl.*, 2017, pp. P.1–P.10.

[91] R. Wang, S. Yuan, C. Liu, D. Guo, and X. Shao, "A three-phase dual-output t-type three-level converter," *IEEE Trans. Power Electron.*, vol. 38, no. 2, pp. 1844–1859, Feb. 2023.

[92] Texas Instruments, "Tida-01606: 10-kW, bidirectional three-phase three-level (t-type) inverter and PFC reference design." 2018. [Online]. Available: https://www.ti.com/tool/TIDA-01606

[93] T. Friedli, M. Hartmann, and J. W. Kolar, "The essence of three-phase PFC rectifier systems–Part II," *IEEE Trans. Power Electron.*, vol. 29, no. 2, pp. 543–560, Feb. 2014.

[94] J. C. Hernandez, L. P. Petersen, and M. A. E. Andersen, "A comparison between boundary and continuous conduction modes in single phase PFC using 600V range devices," in *Proc. IEEE 11th Int. Conf. Power Electron. Drive Syst.*, 2015, pp. 1019–1023.

[95] Y.-S. Kim, W.-Y. Sung, and B.-K. Lee, "Comparative performance analysis of high density and efficiency PFC topologies," *IEEE Trans. Power Electron.*, vol. 29, no. 6, pp. 2666–2679, Jun. 2014.

[96] F. E. U. Reis, R. P. Torrico-Bascopé, F. L. Tofoli, and L. D. S. Bezerra, "Bidirectional three-level stacked neutral-point-clamped converter for electric vehicle charging stations," *IEEE Access*, vol. 8, pp. 37565–37577, 2020.

[97] L. Zhang, X. Yuan, X. Wu, C. Shi, J. Zhang, and Y. Zhang, "Performance evaluation of high-power SiC MOSFET modules in comparison to Si IGBT modules," *IEEE Trans. Power Electron.*, vol. 34, no. 2, pp. 1181–1196, Feb. 2019.

[98] Texas Instruments, "Tida-010210: 11-kW, bidirectional, three-phase ANPC based on GAN reference design," 2022. [Online]. Available: https://www.ti.com/tool/TIDA-010210

[99] M. Safayatullah, M. T. Elrais, S. Ghosh, R. Rezaii, and I. Batarseh, "A comprehensive review of power converter topologies and control methods for electric vehicle fast charging applications," *IEEE Access*, vol. 10, pp. 40753–40793, 2022.

[100] Q.-X. Guan et al., "An extremely high efficient three-level active neutral-point-clamped converter comprising SiC and Si hybrid power stages," *IEEE Trans. Power Electron.*, vol. 33, no. 10, pp. 8341–8352, Oct. 2018.

[101] M. Najjar, A. Kouchaki, J. Nielsen, R. D. Lazar, and M. Nymand, "Design procedure and efficiency analysis of a 99.3% efficient 10 kW three-phase three-level hybrid GaN/Si active neutral point clamped converter," *IEEE Trans. Power Electron.*, vol. 37, no. 6, pp. 6698–6710, Jun. 2022.

[102] Underwriter Laboratories, "Ul 2202: Standard for electric vehicle (EV) charging system equipment," 2018. [Online]. Available: https://www.shopulstandards.com/ProductDetail.aspx?UniqueKey=20342

[103] M. Jahnes, L. Zhou, M. Eull, W. Wang, and M. Preindl, "Design of a 22kW transformerless EV charger with V2G capabilities and peak 99.5% efficiency," *IEEE Trans. Ind. Electron.*, vol. 70, no. 6, pp. 5862–5871, Jun. 2023.

[104] S. Mukherjee, J. M. Ruiz, and P. Barbosa, "A high power density wide range DC–DC converter for universal electric vehicle charging," *IEEE Trans. Power Electron.*, vol. 38, no. 2, pp. 1998–2012, Feb. 2023.

[105] R. A. Friedemann, F. Krismer, and J. W. Kolar, "Design of a minimum weight dual active bridge converter for an airborne wind turbine system," in *Proc. IEEE 27th Annu. Appl. Power Electron. Conf. Expo.*, 2012, pp. 509–516.

[106] J. W. Kolar et al., "Conceptualization and multiobjective optimization of the electric system of an airborne wind turbine," *IEEE Trans. Emerg. Sel. Topics Power Electron.*, vol. 1, no. 2, pp. 73–103, Jun. 2013.

[107] M. Moonem and H. Krishnaswami, "Analysis and control of multilevel dual active bridge dc-dc converter," in *Proc. IEEE Energy Convers. Congr. Expo.*, 2012, pp. 1556–1561.

[108] M. A. Moonem, C. L. Pechacek, R. Hernandez, and H. Krishnaswami, "Analysis of a multilevel dual active bridge (ML-DAB) DC-DC converter using symmetric modulation," *Electronics*, vol. 4, no. 2, pp. 239–260, 2015.

[109] Y. Xuan, X. Yang, W. Chen, T. Liu, and X. Hao, "A three-level dual-active-bridge converter with blocking capacitors for bidirectional electric vehicle charger," *IEEE Access*, vol. 7, pp. 173838–173847, 2019.

[110] A. Agarwal, S. K. Rastogi, and S. Bhattacharya, "Performance evaluation of two-level to three-level three-phase dual active bridge (2l-3 l dab3)," in *Proc. IEEE Appl. Power Electron. Conf. Expo.*, 2022, pp. 361–368.

[111] Wolfspeed, "22 kW bi-directional high efficiency active front end (AFE) converter," 2020. [Online]. Available: https://www.wolfspeed.com/products/power/reference-designs/crd-22dd12n/

[112] Wolfspeed, "25 kW bi-directional active front end (AFE) AC-DC converter reference design," 2022. [Online]. Available: https://www.wolfspeed.com/products/power/reference-designs/crd25ad12n-fmc

[113] Infineon, "11 kW SiC bi-directional DC/DC converter board for EV charging and ESS applications," 2020. [Online]. Available: https://www.infineon.com/cms/en/product/evaluation-boards/ref-dab11kizsicsys/

[114] Wolfspeed, "22 kW bi-directional high efficiency DC/DC converter," 2020. [Online]. Available: https://www.wolfspeed.com/products/power/reference-designs/crd-22dd12n/

[115] M. J. Kasper, J. A. Anderson, G. Deboy, Y. Li, M. Haider, and J. W. Kolar, "Next generation GaN-based architectures: From 240 W USB-C adapters to 11 kW EV on-board chargers with ultra-high power density and wide output voltage range," in *Proc. PCIM Europe; Int. Exhib. Conf. Power Electron., Intell. Motion, Renewable Energy Energy Manage.*, 2022, pp. 1–10.

[116] innoelectric, "On-board charger." [Online]. Available: https://innolectric.ag/on-board-charger-2-2/?lang=en

[117] EDN group, "On-board charger - HPC series." [Online]. Available: https://www.ednqroup.com/products.html?categoria=5

[118] IEEE, "IEEE 519-2014 IEEE recommended practice and requirements for harmonic control in electric power systems," 2014. [Online]. Available: https://standards.ieee.org/ieee/519/3710/

[119] V. Rodriguez, "Automotive component EMC testing: CISPR 25, ISO 11452–2 and equivalent standards," *IEEE Electromagn. Compat. Mag.*, vol. 1, no. 1, pp. 83–90, Jan.–Mar. 2012.

[120] P. S. Crovetti and F. Fiori, "A critical assessment of the closed-loop bulk current injection immunity test performed in compliance with ISO 11452-4," in *Proc. IEEE Int. Symp. Electromagn. Compat.*, 2010, pp. 177–182.

[121] A. Hofer and S. Cecil, "Numerical simulation of field distribution regarding automotive component EMC-testing according to ISO 11452–2," in *Proc. Int. Symp. Electromagn. Compat.–EMC Europe*, 2022, pp. 399–404.

[122] N. A. Thomson, Y. Xiu, and E. Rosenbaum, "Soft-failures induced by system-level ESD," *IEEE Trans. Device Mater. Rel.*, vol. 17, no. 1, pp. 90–98, Mar. 2017.

[123] ISO, "ISO 15118-1:2013, Road vehicles – vehicle to grid communication interface — Part 1: General information and use-case definition," vol. 1, 2013. [Online]. Available: https://www.iso.org/standard/55365.html

[124] N. Keshmiri, D. Wang, B. Agrawal, R. Hou, and A. Emadi, "Current status and future trends of GaN HEMTs in electrified transportation," *IEEE Access*, vol. 8, pp. 70553–70571, 2020.

[125] D. Das, N. Weise, K. Basu, R. Baranwal, and N. Mohan, "A bidirectional soft-switched dab-based single-stage three-phase AC–DC converter for V2G application," *IEEE Trans. Transport. Electrific.*, vol. 5, no. 1, pp. 186–199, Mar. 2019.

[126] H. Belkamel, H. Kim, and S. Choi, "Interleaved totem-pole ZVS converter operating in CCM for single-stage bidirectional AC–DC conversion with high-frequency isolation," *IEEE Trans. Power Electron.*, vol. 36, no. 3, pp. 3486–3495, Mar. 2021.

[127] H. Kim, J. Park, S. Kim, R. M. Hakim, H. Belkamel, and S. Choi, "A single-stage electrolytic capacitor-less EV charger with single- and three-phase compatibility," *IEEE Trans. Power Electron.*, vol. 37, no. 6, pp. 6780–6791, Jun. 2022.

[128] D. Gaona, D. Pauls, and E. F. de Oliveira, "Comparison of dual-active-bridge-based topologies for single-phase single-stage EV on-board chargers," in *Proc. 24th Eur. Conf. Power Electron. Appl.*, 2022, pp. 1–10.

[129] A. K. Bhattacharjee, N. Kutkut, and I. Batarseh, "Review of multiport converters for solar and energy storage integration," *IEEE Trans. Power Electron.*, vol. 34, no. 2, pp. 1431–1445, Feb. 2019.

[130] Y. Tang, J. Lu, B. Wu, S. Zou, W. Ding, and A. Khaligh, "An integrated dual-output isolated converter for plug-in electric vehicles," *IEEE Trans. Veh. Technol.*, vol. 67, no. 2, pp. 966–976, Feb. 2018.

[131] H. Krishnaswami and N. Mohan, "Three-port series-resonant DC–DC converter to interface renewable energy sources with bidirectional load and energy storage ports," *IEEE Trans. Power Electron.*, vol. 24, no. 10, pp. 2289–2297, Oct. 2009.

[132] M. Y. Metwly, M. S. Abdel-Majeed, A. S. Abdel-Khalik, R. A. Hamdy, M. S. Hamad, and S. Ahmed, "A review of integrated on-board ev battery chargers: Advanced topologies, recent developments and optimal selection of FSCW slot/pole combination," *IEEE Access*, vol. 8, pp. 85216–85242, 2020.

[133] S. Haghbin, S. Lundmark, M. Alakula, and O. Carlson, "An isolated high-power integrated charger in electrified-vehicle applications," *IEEE Trans. Veh. Technol.*, vol. 60, no. 9, pp. 4115–4126, Nov. 2011.

[134] W. Taha, P. Azer, A. D. Callegaro, and A. Emadi, "Multiphase traction inverters: State-of-the-art review and future trends," *IEEE Access*, vol. 10, pp. 4580–4599, 2022.

[135] S. Smolenaers, "Methods and systems for an integrated charging systems for an electric vehicle," U.S. Patent US9718370B2, Sep. 24, 2020.

[136] I. Voss, T. Aichinger, T. Basler, P. Friedrichs, and R. Rupp, "Reliability and ruggedness of SiC trench mosfets for long-term applications in humid environment," in *Proc. PCIM Europe; Int. Exhib. Conf. Power Electron., Intell. Motion, Renew. Energy Energy Manage.*, 2018, pp. 1–4.

[137] Wolfspeed, "Discrete silicon carbide mosfets." [Online]. Available: https://www.wolfspeed.com/products/power/sic-mosfets

[138] Qorvo, "Sic fets selector guide." [Online]. Available: https://unitedsic.com/group/sic-fets/

[139] ROHM Semiconductor, "SiC mosfets." [Online]. Available: https://www.rohm.com/products/sic-power-devices/sic-mosfet

[140] Infineon, "Silicon carbide coolsic mosfets." [Online]. Available: https://www.infineon.com/cms/en/product/power/mosfet/silicon-carbide/
[141] GeneSiC, "Discrete silicon carbide mosfets." [Online]. Available: https://genesicsemi.com/sic-mosfet/
[142] R. Pradhan, M. Narimani, and A. Emadi, "Converter topology comparison for a two-stage level-2 onboard charger in 800-V EV powertrains," in *Proc. IEEE IECON–48th Annu. Conf. Ind. Electron. Soc.*, 2022, pp. 1–6.
[143] The British Columbia Hydro and Power Authority (BC Hydro), "Power quality: Energy efficiency reference," 2007. [Online]. Available: https://www.bchydro.com/content/dam/BCHydro/customer-portal/documents/power-smart/business/programs/power-quality-reference-guide.pdf
[144] U. S. Department of Transportation, Bureau of Transportation Statistics, "2021 North American trade value reaches 1.3 trillion, up 8% from pre-pandemic 2019, up 25% from 2020," 2022. [Online]. Available: https://www.bts.gov/newsroom/2021-north-american-trade-value-reaches-13-trillion-8-pre-pandemic-2019-25-2020
[145] M. A. H. Rafi and J. Bauman, "High-efficiency variable turns-ratio semi-dual active bridge converter for a DC fast charging station with energy storage," *IEEE Trans. Transport. Electrific.*, early access, Dec. 23, 2022, doi: 10.1109/TTE.2022.3231554.
[146] O. Zayed, A. Elezab, A. Abuelnaga, and M. Narimani, "A dual-active bridge converter with a wide output voltage range (200–1000 V) for ultra-fast DC-connected EV charging stations," *IEEE Trans. Transport. Electrific.*, early access, Dec. 26, 2022, doi: 10.1109/TTE.2022.3232560.
[147] V. Cirimele et al., "Uncertainty quantification for SAE J2954 compliant static wireless charge components," *IEEE Access*, vol. 8, pp. 171489–171501, 2020.
[148] J. Laskowski, "SAE TIR J2954/2 paves the way for heavy-duty EV charging without a plug & static and dynamic wireless power transfer," *SAE Int.*, 2022. [Online]. Available: https://www.sae.org/news/press-room/2022/12/sae-2022-j2954-2

RACHIT PRADHAN (Student Member, IEEE) received the B.E. degree in electronics engineering from the University of Mumbai, Mumbai, India, in 2018. Since 2021, he has been working toward the M.A.Sc degree focusing on multilevel and multiport DC-DC converters for automotive applications with McMaster University, Hamilton, ON, Canada. From 2016 to 2018, he was the Founder of Pascal Engineering, specializing in engineering consultancy of power electronics, embedded systems, and audio products. From 2018 to 2021, he was a Hardware Design Manager with Maxwell Energy Systems (formerly ION Energy Inc.), specializing in the domain of Li-ion battery management systems. His research interests include system architecture and the development of high-density power electronics for aerospace and industrial applications.

NILOUFAR KESHMIRI (Student Member, IEEE) received the B.Eng. and Management degrees in electrical engineering and management in 2018 from McMaster University, Hamilton, ON, Canada, where she is currently working toward the Ph.D. degree with McMaster Automotive Resource Centre. She has worked on several projects focusing on the design of high performance and efficient power electronic converters for aerospace and electric vehicle applications. She is currently the Project Manager of the McMaster EcoCAR Electric Vehicle Challenge. Her research interests include the design, control, and optimization of power electronics converters in electrified transportation applications. She specializes in high efficiency converter systems using Gallium Nitride (GaN) wide bandgap semiconductor technology.

ALI EMADI (Fellow, IEEE) received the B.S. and M.S. degrees in electrical engineering with highest distinction from the Sharif University of Technology, Tehran, Iran, in 1995 and 1997, respectively, and the Ph.D. degree in electrical engineering from Texas A & M University, College Station, TX, USA, in 2000. He is the Canada Excellence Research Chair Laureate with McMaster University, Hamilton, ON, Canada. He is also the holder of the NSERC/FCA Industrial Research Chair of Electrified Powertrains and Tier I Canada Research Chair of Transportation Electrification and Smart Mobility. Before joining McMaster University, Dr. Emadi was the Harris Perlstein Endowed Chair Professor of engineering and Director of the Electric Power and Power Electronics Center and Grainger Laboratories, Illinois Institute of Technology in Chicago, where he established research and teaching facilities and courses in power electronics, motor drives, and vehicular power systems. He was the Founder, Chairman, and President of Hybrid Electric Vehicle Technologies, Inc. (HEVT) – a university spin-off company of Illinois Tech. He is currently the President and Chief Executive Officer of Enedym Inc. and Menlolab Inc.–two McMaster University spin-off companies. He is the Principal author/coauthor of more than 500 journal and conference papers and several books including *Vehicular Electric Power Systems* (2003), *Energy Efficient Electric Motors* (2004), *Uninterruptible Power Supplies and Active Filters* (2004), *Modern Electric, Hybrid Electric, and Fuel Cell Vehicles* (2nd ed, 2009), and *Integrated Power Electronic Converters and Digital Control* (2009). He is also the Editor of the *Handbook of Automotive Power Electronics and Motor Drives* (2005) and *Advanced Electric Drive Vehicles* (2014). He is the Co-Editor of the Switched Reluctance Motor Drives (2018). Dr. Emadi was the Inaugural General Chair of the 2012 IEEE Transportation Electrification Conference and Expo (ITEC) and has chaired several IEEE and SAE conferences in the areas of vehicle power and propulsion. He was the founding Editor-in-Chief of the IEEE TRANSACTIONS ON TRANSPORTATION ELECTRIFICATION from 2014 to 2020.